

Université du Québec à Chicoutimi

Mémoire présenté à
L'Université du Québec à Chicoutimi
comme exigence partielle
de la maîtrise en informatique

offerte à

l'Université du Québec à Chicoutimi

par

DOU_YANMEI

The Research of the Error Analysis Algorithm with 3D Scanning Data

June 2006



Mise en garde/Advice

Afin de rendre accessible au plus grand nombre le résultat des travaux de recherche menés par ses étudiants gradués et dans l'esprit des règles qui régissent le dépôt et la diffusion des mémoires et thèses produits dans cette Institution, **l'Université du Québec à Chicoutimi (UQAC)** est fière de rendre accessible une version complète et gratuite de cette œuvre.

Motivated by a desire to make the results of its graduate students' research accessible to all, and in accordance with the rules governing the acceptance and diffusion of dissertations and theses in this Institution, the **Université du Québec à Chicoutimi (UQAC)** is proud to make a complete version of this work available at no cost to the reader.

L'auteur conserve néanmoins la propriété du droit d'auteur qui protège ce mémoire ou cette thèse. Ni le mémoire ou la thèse ni des extraits substantiels de ceux-ci ne peuvent être imprimés ou autrement reproduits sans son autorisation.

The author retains ownership of the copyright of this dissertation or thesis. Neither the dissertation or thesis, nor substantial extracts from it, may be printed or otherwise reproduced without the author's permission.

ABSTRACT

With the increase in the automatization level of industrial production, the three-dimensional laser scanning system has been applied in industrial production more and more widely with its advantages of high identification rate, non-destructive capability, and so on. In order to increase the product quality, product testing becomes an important and indispensable link in the industrial production. The research aim of this thesis is, to develop an automatic on-line testing system, based on 3D laser scanner technology. Such a system can contribute to the realization of a complete automatic process from measuring the product to calculating its form error and further judging whether the product is satisfactory or not.

This thesis, starting from the data points obtained from a from 3D scanner, after filtering the noise points in the right and left CCD, makes use of NURBS surface to fit these point data, and reconstruct the surface of the measured object. Based on the principle of the Least Region to assess the form error of the surface, we obtain a mathematic model of the form error of the surface, and further making use an improved Genetic Algorithm, calculate the form error of the object. According to the given acceptable scale of the error, we can judge whether the product is satisfactory or not. Finally, the program design work of the whole system is realized through the use of VC++6.0, with a user interface to calculate form error being implemented.

This research can be applied in the industrial production in order to increase the product quality and the level of automatization. Other potential applications include artificial intelligence, medicine, etc.

Key words: surface fitting, NURBS surface, the Least Region Method, Genetic Algorithm, form error.

ACKNOWLEDGEMENTS

First of all, I would like to express my thanks to my supervisor, Prof. Li-Jun who not only introduced me to this field, but also taught me how to think and analyze the problem. He provided invaluable information and suggestions. I completed this thesis with his generous help and encouragement.

Secondly, I want to give my thanks to Prof. Cao-Zuoliang who helped me master the thesis statement and theory in general, and provided an excellent experimental environment as well as the necessary equipment.

Also, I wish to thank colleagues working with me. With their endeavor and mutual encouragement, I was able to meet the objectives of the thesis.

Meanwhile, my thanks should be given to Tianjin Measurement Center for checking the precision of the experimental setup.

Finally, I must express my special thanks to my parents for providing me a comfortable living environment, which enabled me to pursue this work. They continually encouraged me so that without their help, I might not have finished this thesis.

TABLE OF CONTENTS

ABSTRACT	ii
ACKNOWLEDGEMENTS	iii
TABLE OF CONTENTS.....	iv
LIST OF FIGURES	viii
LIST OF TABLES	x
LIST OF ACRONYMS	xi
CHAPTER 1	1
INTRODUCTION	1
1.1 Research Background and Motivation.....	1
1.2 Research Objective	5
1.3 Research Idea and Main Content of the Thesis	7
1.3.1 Equipment Used in the Research	7
1.3.2 Methodology of the Research	9
1.3.3 Main Content of the Thesis.....	10
CHAPTER 2.....	13
THE MEASURING SYSTEM AND DATA COLLECTION	13
2.1 Measurement of the Actual Object	13
2.1.1 Mapping Function Method of the Least Square Polynomial Regression	16

2.1.2 Testing Straight Line by the Method of Hough Transform	17
2.1.3 Least Square Linear Regression Line	21
2.1.4 Establishing Principle of Mapping Function Relation.....	22
2.2. Point Data Collection and Handling	25
2.2.1 Principle of Sub-pixel	25
2.2.2 Principle of Image Dividing	29
2.2.2.1 Selecting Principle of the Best Scale.....	31
2.2.2.2 Solving the Best Gray Scale with Iterative Method	33
2.2.3 Principle of Stripe Thinning	35
2.2.4 Principle of Image Margin Testing.....	37
2.3 Summary	39
CHAPTER 3	40
THE ALGORITHM OF SURFACE FITTING	40
3.1 Surface Fitting.....	40
3.1.1 Basic Concept of the Spline.....	41
3.1.2 B- Spline Curve	42
3.1.3 Curve of Non-Uniform Rational B-Spline (NURBS).....	44
3.1.4 Surface of Non-Uniform Rational B-Spline	47
3.1.5 NURBS Curve Fitting.....	48

3.1.6 NURBS Surface Fitting	50
3.2 Noise Point of Right and Left CCD Filtering.....	52
3.3 Summary.....	55
CHAPTER 4.....	56
THE CALCULATION OF SURFACE ERROR	56
4.1 Assessing Method of Surface Form Error	57
4.1.1 Definition of Surface Form Error	57
4.1.2 Transformation of 3D Coordinates of the Measured Point.....	58
4.1.3 Calculation of the Smallest Distance from the Measured Point to the Standard Surface.....	60
4.2 Form Error Calculation of the Complex Surface Based on Genetic Algorithm.....	62
4.2.1 Establishment of the Mathematic Model of the Form Error.....	62
4.2.2 Genetic Algorithm of Real Number Encoding	64
4.2.2.1 Genetic Algorithm.....	64
4.2.2.2 Genetic Algorithm of Real Number Encoding.....	66
4.2.3 Calculation of the Surface Form Error	74
4.3 Summary.....	77
CHAPTER 5.....	79
PROGRAM DESIGN AND DATA ANALYSIS	79

5.1 Program Design	79
5.2 Analysis of the Experimental Result.....	83
5.3 Summary.....	91
CHAPTER 6.....	93
THE CONCLUSION AND THE PROSPECTS	93
6.1 Conclusion Remarks	93
6.2 Prospects	99
6.3 Future Work	107
BIBLIOGRAPHY	109

LIST OF FIGURES

Figure 2-1 the 3D laser scanner we use	15
Figure 2-2 parameter space.....	18
Figure 2-3 the corresponding image domain of parameter space.....	19
Figure 2-4 dividing parameter space	19
Figure 2-5 points of space plane	23
Figure 2-6 imaging points of CCD	23
Figure 2-7 regressing two laser lines to locate the characteristic point	24
Figure 2-8 double laser cross-line to decide the characteristic point in CCD	27
Figure 2-9 gray value distribution of double laser image.....	27
Figure 2-10 the laser line that be filtered by row critical value	28
Figure 2-11 the laser line that be filtered by column critical value	28
Figure 2-12 the chart of the best scale	32
Figure 2-13 the distribution of gray value in the image plane.....	36
Figure 3-1 the geometric meaning of weight factor	45
Figure 3-2 the process of the getting parameter of curve	49
Figure 3-3 the error result got through the method without noise point filtering.....	54
Figure 3-4 the error result got through the method with noise point filtering.....	55
Figure 4-1 the definition of surface form error.....	58

Figure 4-2 the cross operation of the unitary real number encoding	72
Figure 5-1 the flow chart of the filtering noise points in left CCD	81
Figure 5-2 the flow chart of surface fitting using NURBS.....	82
Figure 5-3 the experiment of 3D laser scanner.....	84
Figure 5-4 the position of the plane points	86
Figure 5-5 the result of the plane testing	87
Figure 5-6 the position of the standard sphere points.....	88
Figure 5-7 the result of the standard sphere testing	89
Figure 5-8 the position of the free surface points	90
Figure 5-9 the result of the free surface testing	91

LIST OF TABLES

Table 5-1 the results of experiment for the standard sphere	83
---	----

LIST OF ACRONYMS

3D	Three-Dimension
CAD	Computer Aided Design
CAM	Computer Aided Manufacturing
CCD	Charge Coupled Device
CMM	Coordinate Measuring Machine
CNC	Computer Numerical Control
GA	Genetic Algorithm
NURBS	Non-Uniform Rational B-Spline

CHAPTER 1

INTRODUCTION

1.1 Research Background and Motivation

Nowadays, the technology of three-dimensional measurements plays an important role in the field of industrial testing, quality control, machine vision, and so on. It is also an important issue for scientific research on the aspects of analysis, industrial control, biological medicine, material science, and so on. Particularly, the rise of quick shaping and reverse engineering demand more accurate three-dimensional measuring technology for higher automatization and system embedded intelligence ^[37]. One of the methods for three-dimensional scanning measurement is the three-dimensional laser measuring system. It has many advantages such as easy automatization, high measuring efficiency, speed, non-contact, strong anti-jamming power, and so on. Due to these advantages, the three-dimensional laser measuring system has been widely applied in many fields.

Laser scanning measurement is a sort of machine vision, using laser, camera and computer ^[13]. Machine visual measuring technology is a kind of advanced non-contact measuring means with the features of flexible system composition, large work space,

proper precision, and high degree of automation. It is very suitable for online measurement and quality control of industrial site. The measurement of three-dimensional object surface profile is an important means of getting pattern features of the objects. It has great importance and broad applicability in the fields of machine vision, automatic production, industrial testing, and product quality control. Laser non-contact measurement is considered to be the most promising method of three-dimensional measurement, as it has the advantage of high power resolution, non destructive, high data collection speed, and so on^[57]. Three-dimensional laser measurement takes a camera as sensor device and with the help of computer based data processing makes possible the measurement of space position of objects (object point).

Three-dimensional scanning measurement is an extension of the human vision system. With the continuous progress of the research and development of this discipline and the increase of computer processing power, three-dimensional scanning measurement and testing is expected to be applied to more and more complex situations.

Given that competition is ever on the increase, it is becomes important to produce goods in less time and lower cost. The process of testing products has attracted the attention of an increasing number of people. We seek a method guaranteeing the quality of the products which will save time and manpower. The development of three-dimensional laser scanner and computers make this possible. In recent years, with the wider and wider

application scope of industrial automatization and three-dimensional laser scanning technology, product testing has become an indispensable important link in industrial production.

The aim of the testing process is to find the form error. The form error is the main parameter to judge the object's quality. Presently, the methods for measuring form error are mostly confined to simple geometric form. There is not much research on the form error of complex geometric forms. It leads to intricate problems and puts constraints on the development of technology. In the production process, most surfaces are not regular. They are free surface with high variability. The free surface has been found in many fields such as aviation, spaceflight, shipbuilding, automobile and mould industry. And the measuring requirements to achieve efficiency and precision are increasing. The shape of the free surface is very complex, and its measurement method at present for the most part, is based on the coordinates represented by three-coordinate measuring machines. There are some researchers who are now putting forward some methods and means of data handling for the form error of complex surface, based on the Least Region Method, such as the method of approaching linear programming ^[5]. However, the mathematical model to calculate the form error is still very complex. So far, the calculation of the form error of the complex surface, according to the Least Region Method, is still a difficult problem.

Three-dimensional on-line testing is an important approach, and can directly

increase the production efficiency and the quality of products in the industry. Nevertheless, most industries still use manual methods to test the products. This has many disadvantages such as low precision, slow speed, and time consuming. Some industries use contact-measurement machine to test their product with high precision, but with slow speed. This approach needs human intervention. So, it cannot realize on-line automatic testing. Three-dimensional computer based scanning technology can achieve on-line automatic testing.

With the increase of the automatization level of industrial production and the greater level of competition, product quality and work efficiency has become major issues that are of concern to most enterprises. But, at present, most of the production enterprises use the manual method to test the products, which brings many problems, including human error, slow speed, being labor intensive and the impossibility of getting precise information on the products. This will affect the development of the enterprises. This thesis is concerned with the design of a set of system tools for automatically testing form error of products. This system uses a three-dimensional laser scanner to scan a product and to obtain a series of data points. After computer fitting and processing, we obtain the form error of the products. We can then decide whether this product is qualified or not through the form error. This system can implement the complete automatic process from measuring the product to calculating its form error, and further decide whether this product is

qualified or not.

This research can be applied in the industrial production. It will help to increase the automatization level of industrial production, the product precision and the production efficiency, as well as save labor and cost. In this way, the competitive capability of the enterprises will increase. Moreover, the research results can be used in many scientific and application fields, such as artificial intelligence, reverse engineering, automatic aviation, and so on.

The aim of this research is to show the importance of the three-dimensional laser measuring technology in industry and science research.

1.2 Research Objective

In the modern industrial production, the degree of automatization is ever increasing. The product quality is the foundation for the survival of the enterprise. Therefore, product testing becomes an indispensable and important component in industrial production. We have noticed that, at present, the method using manual testing is usually used in industry. There are many indefinite factors in manual testing which can lead to error caused by people. This is a factor to avoid. Even when automatic testing is used; it still cannot automatically finish the whole process from the product scanning to get the form error of product in only one step. Many intermediate processes which can lead to problems exist during the process, which prevents a fully automates industrial testing methodology.

Therefore, this thesis will engage in researching how to get the form error of the measured object automatically and how to really realize the industrial on-line dynamic testing in order to increase the production efficiency and guarantee the product quality.

An additional byproduct of this thesis relates to the profile of the object being measured. These results can be used in many fields. The surface fitting will be involved in all the cases of that using the computer to describe the profile of the object.

The research itself is novel. It combines the originally discrete links together. Many novel algorithms are given, which to some extent, increase the production efficiency and implement fully the automatic testing goal.

Because it is a huge project, many people were needed to finish it together, which means it is a team project. The whole project is divided into the following parts: the scanning of an actual object, getting the data points, pre-handling the point data, CAD modeling, comparing with the standard CAD model of the design, getting the form error and judging whether it is qualified. The main aim of object measurement and testing is to analyze the measured object. The data points we get are discrete, so it is required to do some relevant handling of the data points in order to analyze the object. This thesis is oriented towards constructing an object profile with the data points obtained, and then calculating the form error between the measured object and the standard object in order to judge whether the measured object is qualified.

The thesis designs and implements a set of software tools that can automatically derive the form error of the measured object, and automatically judge whether the object is a qualified product. It realizes the on-line measuring and testing in the industrial production. As already mentioned, this research can be widely applied. As long as the object needs measuring, reconstructing surface and comparing with standard surface are needed. For example, in the context of industrial application, our approach increases the efficiency and precision of industrial production, thus avoiding the error caused by people, saving on the labor force while increasing product quality. In the aspect of robot vision, it can be used to judge the object property that the robot has observed.

1.3 Research Idea and Main Content of the Thesis

1.3.1 Equipment Used in the Research

There are many kinds of different special surfaces in manufacturing, such as automobile frames, precise instruments, toy models, and so on. At present the research is concerned with measuring these surfaces to get relevant data to construct a model for testing. There are two kinds of three-dimensional measurement: contact measurement and non-contact measurement. Between the two, the technology of non-contact measurement has been paid more and more attention to due to its advantages such as no damage, quick speed and high precision.

This thesis taking advantages of advanced laser-based measuring technology realized a completely automated testing of the work pieces.

The equipments of the research are as follows:

- Three-coordinate work station: its function is to move the object to be measured within a certain scope in order that the measured object can be in the correct position for obtaining an image. This involves operating a step motor to obtain a complete three-dimensional coordinate view.
- Laser launcher: it is a critical part of this system. It can give off a hank of laser plane, whose thickness decides the measuring precision. The thinner the laser plane is, the higher the precision will be.
- CCD: two CCD are critical parts of this system also. Together with associated optical lenses, they translate images in each field of vision into the charge signal of CCD, and produce a complete video signal for the follow-up circuit handling. A transfer of the real-timely imagery signal into a computer through data collection card completes the function of image handling.
- Industrial control cabinet: a computer, cooperating with the industrial control cabinet, controls the working power of laser launcher, and brightness and contrast of CCD.
- Computer system and software system: the computer is a common personal computer. There has a EUSYS Picolo data collection card in the computer. Computer and

software system are used to finish the whole data collection and data handling and display the calculating result.

1.3.2 Methodology of the Research

Given the requirements of the project and the actual equipment, the following research ideas and methods were used:

- Making full use of the known conditions: we have already owned a commercial three-dimensional laser scanner. On the basis of the hardware resource, we improved on the critical part (laser probe), while at the same time analyzing relevant algorithms to develop the matching application software.
- Modularity: we did our best to achieve modularization and make each module comparatively independent in order to reduce the restraint among them and increase the algorithm execution time.
- Looking for new algorithm: on the condition of ensuring the precision and speed, we looked for a new plan and new algorithms. At the same time part solving the problem, implied further simplification of the operation, thereby adding to the flexibility and practicability. We also tried to enlarge the scope of applications.

This thesis is a continuation of previous works. We mention the work of Wang-Shu and Lin-Yibin. They improved the hardware of 3D laser scanner to enhance its precision. They also designed software which displays information of data points of the products on

computer screen. The data points collected were based on the 3D laser scanner that had been improved by them.

Using principle from optics, mathematics, measurement, and computer science, the present thesis realizes the automatic calculation of form errors. There is some originality in the theory and algorithms:

- Creatively giving the method of filtering the noise in the double CCD.
- Deriving a method that calculates the distance from the point to the standard surface.
- Creatively combining the NURBS surface fitting, the Least Region Method and the Genetic Algorithm together. The Genetic Algorithm used was improved and generates results with high precision.
- Design of the software with a user interface for form error measuring.

The research on those problems can lead to promoting the application of laser vision in the fields of industrial measurement and testing, body measurement, disable limb resuming, pattern analysis, artificial intelligence and city digital construction, and so on.

1.3.3 Main Content of the Thesis

The thesis is composed of six chapters. The content is as follows:

- Chapter 1 introduces the basic ideas, theoretical system, development and application of three-dimension scanning measurement and testing. The research motivation,

objectives, ideas, methods, main content and the structure of the whole thesis are also introduced.

- Chapter 2 introduces the hardware equipments of the object measuring used in the whole measuring and testing system, and the main theory of data collection. It also introduces how the three-dimensional scanner scans the objects and transforms the information of the objects into the form of three-dimensional data point which are then stored in the computer.
- Chapter 3 introduces the method of NURBS used for surface fitting of the object, and gives specific fitting method and formula. Completing the surface reconstruction of the object is also discussed and we give a new method of filtering the noise component of the data points.
- Chapter 4 introduces the method used to calculate the form error between the measured surface and the standard surface. We make use of the principle of the Least Region to establish the mathematical model of the form error, and realize the final calculation with the Genetic Algorithm.
- Chapter 5 introduces the relevant task of software design and the user interface displayed. Experiments prove the feasibility and practicality of this research to get satisfactory results.
- Chapter 6 concludes the research results and main content of this thesis and

discusses potential future work.

CHAPTER 2

THE MEASURING SYSTEM AND DATA COLLECTION

This project uses the basis of 3D laser measurement. We obtain three-dimensional data points of an object using a 3D laser scanner, and then using these data points, fit a surface to the object. Using the Least Region Principle and a Genetic Algorithm, we get the form error of the object, and then according to this form error, judge whether the product is qualified or not thereby implementing an on-line dynamic testing tool. It can be said that, the design of the measuring system and the precision of data collection are the necessary parts of the whole project. They are also important links of the whole project that will affect the final result. This chapter introduces the relevant work and principles of the object measuring and data collection.

2.1 Measurement of the Actual Object

With the development of industrial automation, 3D measurement has been used more widely. Many companies have improved on the technique of 3D measuring machines. This has led to the manufacture of more advanced machines. It makes measurement of the three-dimensional object easier to operate with better precision. The earliest Coordinate

Measuring Machine was manufactured by Japan in 1968. And then, the Rolls Royce Company produced contact probe in 1971.

Coordinate Measuring Machine can measure 3 directions of objects including length, width and height.

At present, the CMM (Coordinate Measuring Machine) includes two primary categories. They are contact measuring machine and non-contact measuring machine. The 3D laser scanner is a type of non-contact measuring machine. The advantages of 3D laser scanner are ^[58]:

- It need not do compensation of probe's radius.
- Measurement's speed is very fast. It need not measure points one by one as contact measurement does.
- Soft objects, thin objects and high degree precision objects that cannot be contacted can be measured directly. This advantage allows for the measurement of deleterious objects and brittle objects. It has many advantages over other techniques.

Three-dimensional laser scanner offers one effective method to measure 3D objects. It can gather the points accurately and quickly. And it simplifies the process of measurement. It no longer requires skillful operators. Any operators can use it easily.

The probe of 3D laser scanner is CCD (Charge Coupled Device). It can measure objects fast and accurately. It is good at changing objects frequently ^[56]. The probe can

gather the coordinates of points. Using these points, the computer can analyze and compute the result.

We designed a set of visual sensors used for testing by ourselves. We used this machine and established a visual measuring system for scanning an object and analyzing the information of the points.



Figure 2-1 the 3D laser scanner used

2.1.1 Mapping Function Method of the Least Square Polynomial Regression

In order to avoid the cumbersome procedures of parameter demarcation, we will handle the demarcation of parameter in the system with a hidden method, and thus simplify the measuring algorithm. We take the Mapping Function Method as the algorithm of visual testing.

The basic problem of the measurement is how to converse the image coordinates in CCD camera into space coordinates of the entity. Each characteristic point $K(u_k, v_k)$ in CCD image maps corresponds to the point (S_k, R_k) in the space graphic. Through these discrete points, we can use polynomial regression to show their relationships:

$$\begin{cases} R(u, v) = \sum_{j=0}^n \sum_{i=0}^{n-j} c_{ij} u^i v^j \\ S(u, v) = \sum_{j=0}^n \sum_{i=0}^{n-j} d_{ij} u^i v^j \end{cases} \quad (2-1)$$

The error function E_R and E_S of $R(u, v)$ and $S(u, v)$ are:

$$\begin{cases} E_R = \sum_{k=0}^m (R_k - R)^2 \\ E_S = \sum_{k=0}^m (S_k - S)^2 \end{cases} \quad (2-2)$$

Therefore, regression coefficient c_{ij} and d_{ij} can be obtained by the method of Least Square Regression, i.e.

$$\begin{cases} \frac{\partial E_R}{\partial c_{ij}} = 0 \\ \frac{\partial E_S}{\partial d_{ij}} = 0 \end{cases} \quad (2-3)$$

Solving the equation yields the regression coefficient, which enable the whole mapping relation to be completely established. After this regression polynomial calculation, any measuring point can get its corresponding space coordinates (S, R) through its image coordinates (u, v) .

2.1.2 Testing Straight Line by the Method of Hough Transform

In the process of the design of visual sensor and the following visual testing, it is inevitable to use some critical visual testing technology^[11]. In the process of actual testing, it uses the non-sensitivity of Hough Transform^[10], and improves Hough Transform to filter out useless noise, and then uses the method of the Least Square Linear Regression to increase the linear regression precision. Thus, the testing accuracy of the straight line will increase and the accurate location of the intersection of laser cross line will be realized.

In essence, Hough Transform is a conversion equation of image space and parameter space. The basic principle is as following^[28]. The linear equation is:

$$r_0 = x \cos \theta_0 + y \sin \theta_0 \quad (2-4)$$

It corresponds to a point (r_0, θ_0) in parameter space (r, θ) . Meanwhile, each point (x_0, y_0) in the straight line corresponds to a curve $r = x_0 \cos \theta + y_0 \sin \theta$ in

parameter space. Thus, the n points in the straight line correspond to n curves in parameter space. These n curves in parameter space all will go through one point (r_0, θ_0) . Thus, through finding the point (r_0, θ_0) in the parameter space we will get the linear equation.

The traditional Hough Transform takes each point of the image into the formula (2-4). Calculating the result implies voting in the parameter space. The parameter of the point getting the most votes will be taken as the corresponding parameter of the required straight line in the parameter space. We use an improved algorithm to solve the straight line.

The principle is as the following:

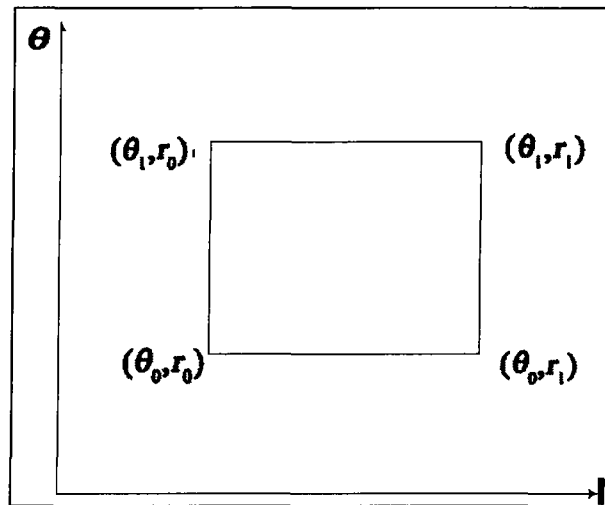


Figure 2-2 parameter space ^[26]

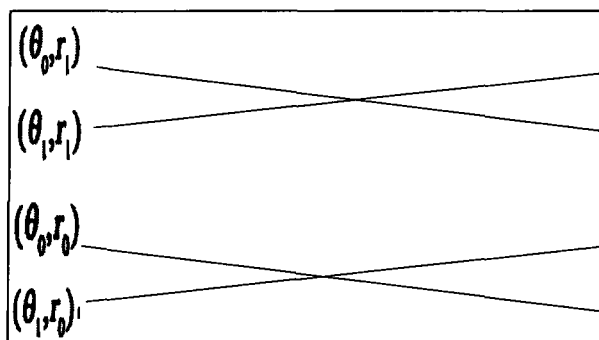


Figure 2-3 the corresponding image domain of parameter space ^[26]

A point (r_i, θ_i) in parameter space corresponds to a straight line in image space. A tiny rectangle domain (Figure 2-2) in parameter space will correspond to a domain of X shape (Figure 2-3).

If the rectangle domain is very small, approaching to an individual pixel, then the domain of X shape in image space will approach to a straight line. The specific algorithm is as following (Figure 2-4):

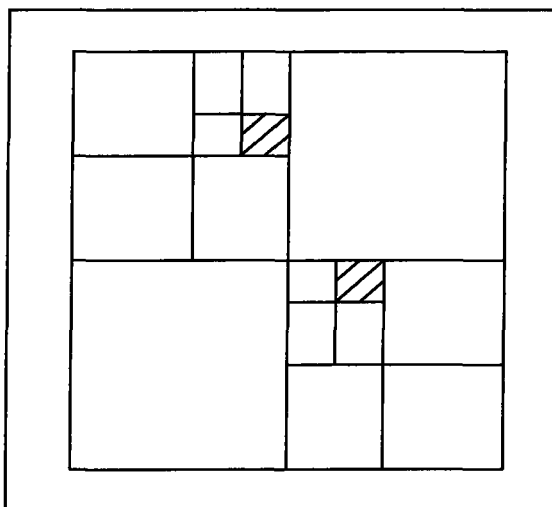


Figure 2-4 dividing parameter space

Take the whole parameter space as a unit, calculate out its corresponding domain in image space; solve the number of the corresponding image points L in this region. If L is less than some threshold T initially set (the least number of the points in the straight line), it means that the straight line does not exist and the operation is suspended; if L is more than threshold T , then it required to further divide this unit into four parts (the size may not be exactly the same). Then, test whether the size of the further divided unit are less than D_{\min} . If it is, the search is suspended; If not, then take the further divided unit, and find out the corresponding L ; if L is less than T , then turn to find the next unit of the same level; if L is more than T , then it needs to further divide the present unit and find one by one.

Accordingly, the search will not suspend until the size of the present unit is less than D_{\min} . Record all the position of units satisfying $L > T$ at this moment, and meanwhile, save the coordinates of image points corresponding to these units. In order to find the precise parameter of straight line, we need to divide the units that got through the operation mentioned above further into $N \times N$ small units (in the experiments, N is 10). According to the image points included in the present units vote for each small unit and record the votes. Find the unit where the center is, and take the center point of the unit as the parameter of the straight line.

This method can quickly filter the great amount of non-straight points in space, and

quickly find the corresponding points of the straight line, which shorten the calculating time and save the memory at the same time ^[53]. Compared with the traditional Hough Transform, it can divide the parameter space more finely and record each parameter space and its corresponding point group. Further test these point groups, then the obtained parameter will be more precise.

2.1.3 Least Square Linear Regression Line

After the filtering of Hough Transform, the group of information points basically belongs to straight lines. At this moment, we use Least Square Linear Regression to make the regression parameter of the straight line more precise. The final testing precision will be better than 0.1 pixels.

The regression function is shown as following:

$$\mu(x) = a + bx \quad (2-5)$$

Make use of the Least Square Method to estimate parameters a and b , and suppose that y_i submitting to Normal Distribution $N(a + bx_i, \sigma^2)(i = 1, 2, \dots, n)$, and solve the function 2-6 respectively.

$$S = \sum_{i=1}^n (y_i - a - bx_i)^2 \quad (2-6)$$

Solve the partial derivative of a and b , and order them to be zero, and then we can get the equation as the following:

$$\begin{cases} na + \left(\sum_{i=1}^n x_i \right) b = \sum_{i=1}^n y_i \\ \left(\sum_{i=1}^n x_i \right) a + \left(\sum_{i=1}^n x_i^2 \right) b = \sum_{i=1}^n x_i y_i \end{cases} \quad (2-7)$$

The results are as following:

$$\begin{cases} \hat{a} = \bar{y} - \hat{b}\bar{x} \\ \hat{b} = \frac{l_{xy}}{l_{xx}} \end{cases} \quad (2-8)$$

Hereinto:

$$\bar{x} = \frac{1}{n} \sum_{i=1}^n x_i, \quad \bar{y} = \frac{1}{n} \sum_{i=1}^n y_i \quad (2-9)$$

$$l_{xy} = \sum_{i=1}^n (x_i - \bar{x})(y_i - \bar{y}) = \sum_{i=1}^n x_i y_i - n\bar{x}\bar{y} \quad (2-10)$$

$$l_{xx} = \sum_{i=1}^n (x_i - \bar{x})^2 = ns_x^2 \quad (2-11)$$

And, s_x^2 means square deviation of x_1, x_2, \dots, x_n .

The linear equation $\hat{y} = \hat{a} + \hat{b}x$ is called the linear regression equation. And \hat{b} is regression coefficient and the corresponding straight line is regression straight line.

2.1.4 Establishing Principle of Mapping Function Relation

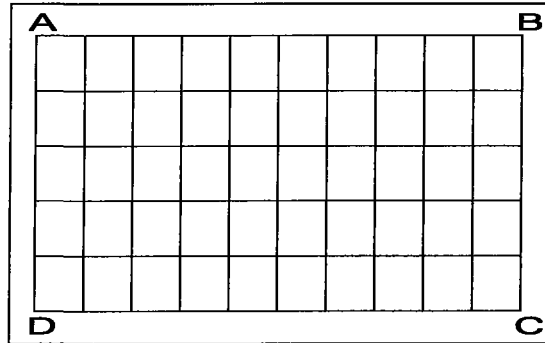


Figure 2-5 points of space plane

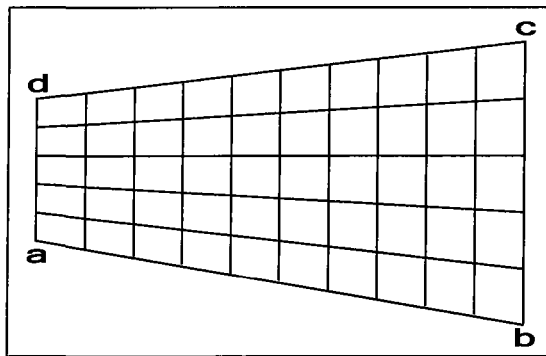


Figure 2-6 imaging points of CCD

Establishing the mapping relationship between the points of the space plane (Figure 2-5) and the imaging points of the CCD (Figure 2-6) is the most important step to use the Mapping Function Method. Because the characteristic points are distributed in a lattice shape, the imaging cannot be a single pixel. It is required to find the center of these characteristic points from a set of bright spots. Here, we use the cross point of two laser straight lines to locate the characteristic point. For the straight line, filter the point with Hough Transform and then make use of the Least Square Regression to fit the equation of

the straight line. Thus, we can find the position of the characteristic point in the CCD image space more precisely. The degree of precision can be of the order of one of 0.1 pixels (shown as in the Figure 2-7).



Figure 2-7 regressing two laser lines to locate the characteristic point

Supposing the two equations regressed by the straight line are as following:

$$\begin{cases} v_m = au_m + b \\ v_n = eu_n + f \end{cases} \quad (2-12)$$

Then the coordinates (u_p, v_p) of the intersection p of sub-image are:

$$\begin{cases} u_p = (f - b)/(a - e) \\ v_p = (af - be)/(a - e) \end{cases} \quad (2-13)$$

Therefore, the image coordinates (u_p, v_p) of any point in CCD image space can be decided in such a way, and mapped into the space coordinates (S_p, R_p) . Its precision can

reach the level of sub-pixel. After establishing the relationship of the two, it is possible to use the mapping relation to scan the three-dimensional surface of the object.

2.2. Point Data Collection and Handling

Based on the principle of measurement and combining the knowledge of image handling, numerical statistics and physiology, we have established a laser visual on-line measuring system. We researched how best to solve the critical and technological problems associated with slow speed, low precision in the laser visual measuring. Combining many principles, we use the iterative method of Histograms to solve the best scale, and Center of Surface Method to thin stripe, and Canny Operator to test edge.

2.2.1 Principle of Sub-pixel

Because general video information takes pixel as unit, pixel point will constrain information analysis. Therefore, we researched the mapping function of sub-pixel point regression, with the hope of increasing the precision of the present measuring through the method of sub-pixel analysis.

In 1930, Schmaltz first put forward the method of using projection beam to measure shape surface. The sampling and record of surface should be up to the precision of 0.2mm. An object of 200mm×200mm should provide the analysis ability of 1000×1000 pixel point within this visual region. This case will result in too many points which are

unacceptable. The alternative method is to reconstruct the profile in the same CCD, through adjusting the ability of space analysis properly, and under the condition of the same precision using apparent reduced data. If Laser beams can be handled by simple images, especially when the distribution of gray value is linearly increased, the points of profile will get space division of 1/10 pixel point. If it is so, in the requirement of the same precision, it can be got through 100×100 pixel points. This is the concept of sub-pixel point.

The approach taken uses line laser as light source, through a CCD to get the video of laser beam cross section. With the assistance of precise location and the horizontal moving function provided by CMM, and utilizing the coordinates of each pixel point in CCD camera and the relationship with its corresponding coordinate system, we get a more precise 3D profile.

The method of using double laser cross-line to locate characteristic point can increase the location ability of standard characteristic point through the analysis ability of sub-pixel. The produced result of the image of double laser cross-line is shown in the Figure 2-8. Through calculating the coordinates of image points of the same x coordinates with the principle of superposition, the gray value distributing chart of each line as shown in Figure 2-9. As the horizontal axis shown in Figure 2-9, through selecting proper critical value, we can clear the whole image line whose statistical value is more than critical value,

and then the horizontal laser image will be obtained as is shown in Figure 2-10. In the image, we called the point whose gray value is more than critical gray value as effective point. It is set as laser line $t t'$. The image coordinates of each effective point on the line is set as (x_t, y_t) . With the principle of the superposition to calculate a gray value, another group of vertical image line $v v'$ can be obtained as shown in the Figure 2-11.

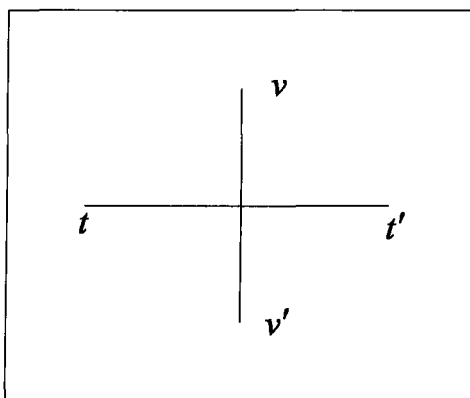


Figure 2-8 double laser cross-line to decide the characteristic point in CCD

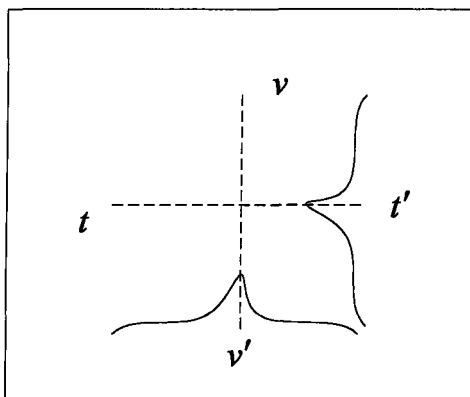


Figure 2-9 gray value distribution of double laser image

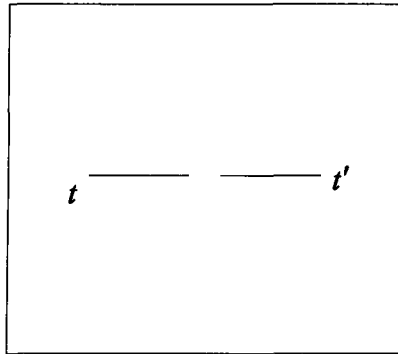


Figure 2-10 the laser line that be filtered by row critical value

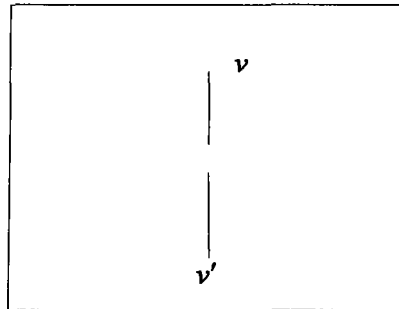


Figure 2-11 the laser line that be filtered by column critical value

The image coordinates of each effective point on the vertical direction is set as (x_v, y_v) . And then using the analysis theory of the Least Regression to find the intersection P of the two line groups, the precision of sub-pixel can be achieved. Supposing the equation of line $t t'$ is expressed as $y_t = a \times x_t + b$; and the equation of line $v v'$ is expressed as $y_v = e \times x_v + f$; and the corresponding error functions of E_t and E_v of line $t t'$ and line $v v'$ are expressed respectively as the following:

$$\begin{aligned}
E_t &= \sum_{i=1}^u (y_{ti} - a \times x_{ti} - b)^2 \\
E_v &= \sum_{i=1}^w (y_{vi} - e \times x_{vi} - f)^2
\end{aligned} \tag{2-14}$$

Solving the equation, we got:

$$\frac{\partial E_t}{\partial a} = 0, \quad \frac{\partial E_t}{\partial b} = 0 \tag{2-15}$$

Then the factors of a and b can be obtained, and solving the equations:

$$\frac{\partial E_v}{\partial e} = 0, \quad \frac{\partial E_v}{\partial f} = 0 \tag{2-16}$$

The factors of e and f can be got, then the coordinates (x_p, y_p) of point P of sub-pixel point:

$$\begin{aligned}
x_p &= (f - b)/(a - e) \\
y_p &= (a \times f - b \times e)/(a - e)
\end{aligned} \tag{2-17}$$

If the space coordinates of point P are (S_p, R_p) , then the relation of image coordinates (x_p, y_p) of CCD image mapping into the space coordinates (S_p, R_p) can be established.

2.2.2 Principle of Image Dividing

In the application research on the analysis and handling of the image, people are always interested in some “meaningful” region, i.e. some special regions with unique characteristic in the image. These regions are defined target, and other parts are called background. In order to identify and analyze the target, it needs to separate and extract

these regions from the image^[24]. This is the technology of image dividing. The selecting of the features can be one of gray, shape gene, veins, and so on. There are many methods for image dividing. The classic methods are like the method of dividing based on histograms of pixel, the region growing method based on neighbor region, and so on. In recent years, many new methods have appeared continuously, such as the dividing technology based on the analysis and transform of the wavelet, and the dividing technology based on mathematic morphology, and so on.

The scale method is a kind of image dividing method most often used. The image scale dividing consists in dividing the image space into some meaningful regions according to the scale. The basic idea is that of making use of the gray characteristic of the image to select one (or more) optimal gray scale, and comparing the gray value of each pixel and each scale in the image. We think that the pixels belonging to the same part are in the same object^[33].

The advantages of the scale dividing method are^[45]: (1) the principle is clear and easy to understand; (2) the realization of the algorithm is simple and clear; (3) the dividing effect is good. Taking the efficiency (dividing effect/ operation) into consideration, the scale dividing is indeed the best choice.

The scale transform of gray can transform an image into the two-value image with black and white. Its operation process is that, first the users appoint a scale or get a scale

automatically through calculation; if the gray value of some pixel is less than the scale, set the gray value of this pixel is 0; or else, set the gray value of this pixel is 255.

The expression of the transform function of the gray transform is as following:

$$f(x) = \begin{cases} 0 & x < T \\ 255 & x \geq T \end{cases} \quad (2-18)$$

Where T is the appointed scale.

2.2.2.1 Selecting Principle of the Best Scale

Scale is an important technology in the image dividing approach. The traditional method is to select the scale according to the one-dimensional histograms of gray. The users appoint directly the scale generally obtained by experience or experiments. This can guarantee less procedure code and quick operation speed. But its applicable field is too small. If the work environment of the measuring system can stay the same, this method can be used; or else, we need to find other method.

The so-called beat scale means the scale that can get the smallest error of the target and background. Supposing an image is composed of a dismal target object and the bright background as the Figure 2-12 shows, and we know that the density functions of their distribution probability of gray degree respectively are $p_1(Z)$ and $p_2(Z)$; the proportion of the number of the target pixels in the whole image is θ ; then the general density functions of the distribution probability of gray degree $p(Z)$ can be expressed as following:

$$p(Z) = \theta p_1(Z) + (1 - \theta) p_2(Z) \quad (2-19)$$

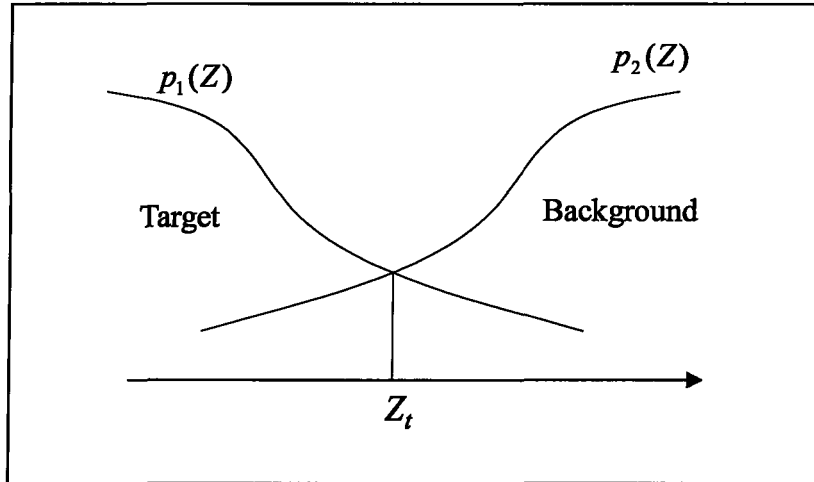


Figure 2-12 the chart of the best scale

If selecting Z_t as scale, then the general error probability $E(Z_t)$ is:

$$E(Z_t) = (1 - \theta)E_1(Z_t) + \theta E_2(Z_t) \quad (2-20)$$

In the formula :

$$E_1(Z_t) = \int_{-\infty}^{Z_t} p_2(Z) dZ \quad (2-21)$$

$$E_2(Z_t) = \int_{Z_t}^{\infty} p_1(Z) dZ \quad (2-22)$$

The best scale is Z_t when $E(Z_t)$ is minimum, for the formula (2-20), applies

Liebnitzs Rule, then there is:

$$\theta p_1(Z_t) = (1 - \theta) p_2(Z_t) \quad (2-23)$$

Just supposing $p_1(Z)$ and $p_2(Z)$ are Normal Distribution functions, and their gray average are respectively μ_1 and μ_2 , and the standard deviations of gray average are

respectively σ_1 and σ_2 , and then there is:

$$p_1(Z) = \exp\{[-(Z - \mu_1)^2]/(2\sigma_1^2)\}/(\sqrt{2\pi}\sigma_1) \quad (2-24)$$

$$p_2(Z) = \exp\{[-(Z - \mu_2)^2]/(2\sigma_2^2)\}/(\sqrt{2\pi}\sigma_2) \quad (2-25)$$

Put the formulas (2-24) and (2-25) into the formula (2-19), and then solve the logarithm in both sides:

$$AZ_i^2 + BZ_i + C = 0 \quad (2-26)$$

In the formula:

$$A = \sigma_1^2 - \sigma_2^2$$

$$B = 2(\mu_1\sigma_2^2 - \mu_2\sigma_1^2)$$

$$C = \sigma_2^2\mu_2^2 - \sigma_2^2\mu_1^2 + \sigma_1^2\mu_2^2 \ln(\sigma_2 p_1 / \sigma_1 p_2)$$

$$p_1 = \theta$$

$$p_2 = 1 - \theta$$

The formula (2-26) is the quadratic equation of Z_i , whose positive solution is the best scale.

2.2.2.2 Solving the Best Gray Scale with Iterative Method

For the image of single object, supposing the gray degree of the object and the background is the Normal Distribution. Transform the formula (2-26) into:

$$-Z_i^2 + bZ_i + c = 0 \quad (2-27)$$

In the formula: $b = B/A$, $c = C/A$, then we can deduce the iterative formula:

$$Z_t = \sqrt{bZ_t + c} \quad (2-28)$$

Taking the original scale is Z_{t0} (it can be taken by any scale calculating method), and put it into the above formula to iterative compute (every time it needs to recalculate the parameter b and c). The iterative process will not stop until the following formula is be satisfied:

$$\left| Z_t - \sqrt{bZ_t + c} \right| < \varepsilon \quad (2-29)$$

Here, ε is the appointed small positive number.

It needs to recalculate parameters b and c every time. Here, it only need to recalculate $\mu_1, \mu_2, p_1, p_2, \sigma_1, \sigma_2$. We can approximately view μ_1 and μ_2 as the corresponding gray value of the two peak value in the histograms. We can get p_1 and p_2 through calculating the number of the pixels of the object and the background. Supposing $n(z)$ is the number of the pixels whose gray value is z . It can be got through histograms.

When the scale is Z_t , the number of the pixels of the object is:

$$n_1 = \sum_{-\infty}^{Z_t} n(z) \quad (2-30)$$

The number of the pixels of the background is:

$$n_2 = \sum_{Z_t}^{+\infty} n(z) \quad (2-31)$$

And then

$$p_1 = n_1 / (n_1 + n_2) \quad (2-32)$$

$$p_2 = n_2 / (n_1 + n_2) \quad (2-33)$$

The square deviation can be approximately got through histograms:

$$\sigma_1^2 = 2 \sum_{z=-\infty}^{z_1} (z^2 \frac{n(z)}{n_1}) - \mu_1^2 \quad (2-34)$$

$$\sigma_2^2 = 2 \sum_{z=z_1}^{+\infty} (z^2 \frac{n(z)}{n_2}) - \mu_2^2 \quad (2-35)$$

If there are two or more than two objects in the images to be divided, the histograms of the image are multi-apex shape. At this moment, take one object corresponding to the most prominent apex in the histograms as “object”, and all other objects and background are “background”. Take out the “object” with the scale selecting method stated previously, and then the dividing of the first object is finished. And then it can imitate this process to take out all the other objects.

2.2.3 Principle of Stripe Thinning

For a CCD measuring system with a resolving power of 512×480 , if its measuring scope in the x direction is 52.2mm, the resolving power of one pixel in x direction is only 0.1mm/pixel. That means, if only the width of the stripe rays is more than 0.1mm, there will be more than two pixels that can feel the signal. Therefore, it is a problem that cannot be ignored, that of finding the proper thinning stripe in these pixels.

Because the stripe ray has width, the luminosity reflecting on the object surface will

be attenuated. When the stripe light hits the object, the partial gray value distribute in the x -axis as the Figure 2-13 shows, which stands for the brightness distribution of a ray belt in some cross section, similar to a Gauss Distribution. Therefore, there are two kinds of center algorithm that are the most common and simple: the largest bright-point method and center of surface method. The largest bright-point method is, that for each line in the CCD image plane, scanning orderly and comparing the maximum of the brightness in each line, and then ranking out. This is the stripe center of this ray belt. The center of surface method is, that for each line in the CCD image plane, scanning orderly and then according to the Center of Surface Principle calculating the center coordinates (X_g, Y_g) of each line and then ranking out orderly.

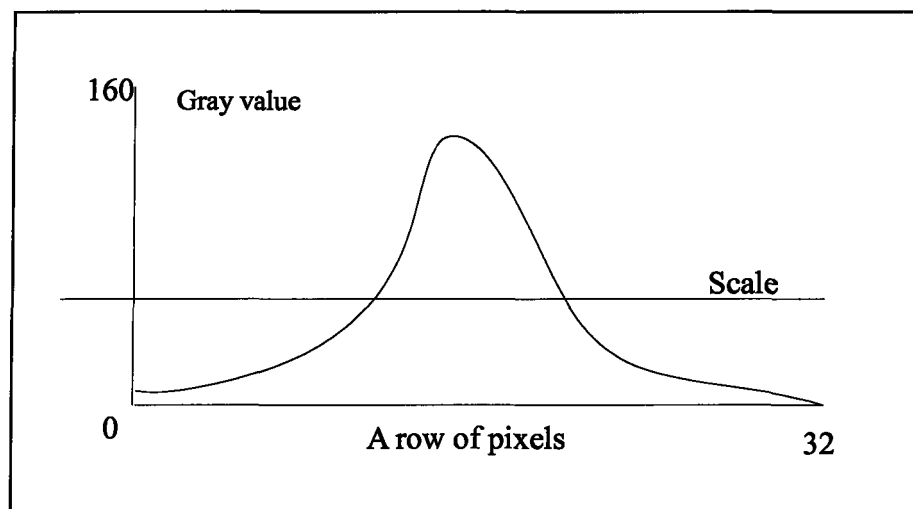


Figure 2-13 the distribution of gray value in the image plane

Regardless of which method used, it must make use of the best scale selecting method stated previously to get the dividing scale in order to filter the noise points with the

smaller gray value. Besides, there are some other thinning algorithms, such as the handling algorithm based on mathematical morphology, and so on.

2.2.4 Principle of Image Margin Testing

There are two steps that the human visual system employs to recognize a target: first, it must separate the image margin and the background, which has been stated previously; and then the detail of the image can be recognize from the profile of the image [36]. The computer vision is just imitating the process in human vision. Therefore, when testing the object margin, first it needs to test its profile point briefly and then join the originally tested points. Meanwhile, the missed marginal points are tested and joined, and also the in- veracious marginal points can be take off.

The margin widely exists between objects and background, object and object, the unit and unit. Therefore, it is important feature that the image dividing depends on, is the basis of computer vision and mode identification, and so on, and is also an important part in image division. However, margin testing is a difficult problem in image dividing. Because the margin of actual image is always the combination of various types of margins, and also because there is noise in the actual image signal, noise and margin are both signals of high frequency. It is difficult to make a choice with bandwidth.

If a pixel is in the margin of some object in the image, then its neighbor region will become a changing belt of gray degree. For this kind of change, the most useful features

are the changing rate and the direction of the gray.

The margin-testing operator tests the neighbor region of each pixel and calculates the changing rate of gray also including the determination of direction.

There are many basic algorithms of the margin testing, such as Gradient Operator, Direction Operator, Laplacian ^[2] and Canny Operator ^[6], and so on. What this thesis uses is Canny Operator.

The essence of Canny Operator is using one associate Gauss Function $f_s = f(x, y) \times G(x, y)$ to do smooth calculation, and then locating the maximum of differential coefficient using Differential Operator.

After smoothing, the gradient of $f_s = f(x, y)$ can use the approximate formula of 2×2 differential with one rank:

$$\begin{aligned} P[i, j] &\approx (f_s[i, j+1] - f_s[i, j] + f_s[i+1, j+1] - f_s[i+1, j]) / 2 \\ Q[i, j] &\approx (f_s[i, j] - f_s[i+1, j] + f_s[i, j+1] - f_s[i+1, j+1]) / 2 \end{aligned} \quad (2-36)$$

In this formula, solving the average of differential is convenient for calculating the deviated differential coefficient gradient of x and y in the same point. The extent value and the direction angle can be calculated by the transform the coordinates to polar coordinates:

$$\begin{aligned} M[i, j] &= \sqrt{P[i, j]^2 + Q[i, j]^2} \\ Q[i, j] &= \arctan(Q[i, j] / P[i, j]) \end{aligned} \quad (2-37)$$

The margin intensity of the image is reflected by $M[i, j]$; Direction of the margin is

reflected by $\theta(i, j)$. When $M[i, j]$ is maximum, the direction angle $\theta(i, j)$ reflects the direction of the margin.

2.3 Summary

This chapter introduced the relevant task and the main principles components of the present work and involved primarily object measurements and data point collection. Because the surface fitting of the measured object and the calculating of the form error are both based on the three-dimensional data points, the task of data point collection is more important.

Tianjin Measurement Center has validated the precision of the systems we use, and the result shows that the precision of this system is indeed quite satisfactory. Therefore, we can use the data point obtained using this system to finish the task of this thesis.

CHAPTER 3

THE ALGORITHM OF SURFACE FITTING

Now, that we have obtained many data points from the 3D scanner, the task of this chapter is to handle these points and use them to fit the surface of the measured object. As a result of surface fitting, the computer can reconstruct the profile of the object, and show the object in computer. In order to increase the precision, the noise point obtained from the double CCD measuring system must be subtracted.

3.1 Surface Fitting

The objective of surface fitting is to find some mathematic model that can express a given shape of the object accurately and simply. And using the surface fitting, we can analyze, calculate, and modify the surface^[38].

There are many methods for surface fitting. Because the same information may be recorded repeatedly, the method of Cubic Spline function is not suitable^[41]. The curve fitted by this method will go through all points and make mistake when information is repeated. While among the methods that the fitted curve will not go through all points, because of too strong pertinence among points, if the error of one point of Bezier curve is

too large^[27], it will affect the fitted result. The method of B-Spline shows strong power in expressing and designing free curve and surface^[49], but it encounters some trouble in expressing and designing the primary curve and surface. B-Spline surface cannot precisely express the conicoid except paraboloid, but can only give the approximate expression. The method of the Non-Uniform Rational B-Spline (NURS), is mainly to find out the mathematical method that is uniform with the method of B-Spline and can also precisely express conicoid^[9].

The main advantages of the method of NURBS:

- It provides a public mathematic form for the precise description of both standard shape (the primary curve and surface mentioned above) and free curve and free surface^[25].
- It corrects controlling peak and weighs to design all kinds of surface flexibility.
- It has obvious geometric explanation and powerful technology of geometric (including node inserting, subdividing and up-ordering, and so on.)
- It is unchangeable to geometric transformation and projection transformation.
- There are some special cases, such as the methods of Non-rational B-Spline^[30].

There is only one method to fit the surface in the standard of STEP^[35]. It is NURBS.

3.1.1 Basic Concept of the Spline

Before making use of computer automatic drawing, in the fields of aviation,

automobile, and shipping manufacturing, the spline is often used to map free curve manually ^[54]. The spline is a thin batten (metal or plexiglass) with flexible and well-proportioned texture. It can, according to the requirements and through a group of appointed points, produce smooth curve. When drawing, the draftsman uses iron to pressure elastic spline in order to make it go through the appointed points. The draftsman can change spline shape by adjusting the weight of the pressed iron properly, in order to achieve the required shape of design, and then, along the spline draw the required smooth curve, and this is spline curve.

The produced curve applying this kind of spline tool is very smooth. Therefore, people try to find mathematic model to describe the curve by this kind of spline tool ^[23]. In computer graphics, spline curve means the joining multinomial curve segments, satisfying the special continuity condition at the end point of each segment of the curve or surface ^[43]. Spline surface is described by two groups of orthogonal spline curves.

3.1.2 B- Spline Curve

B-Spline curve use the controlling point to get controlling polygon, and then produce curve, in order to get the geometric shape of the curve ^[7].

The formula of k-order B-Spline curve is as following:

$$P(t) = \sum_{i=1}^{n+1} N_{i,k}(t) V_i \quad t_{\min} \leq t < t_{\max}, \quad 2 \leq k \leq n+1 \quad (3-1)$$

$$N_{i,l}(t) = \begin{cases} 1 & x_i \leq t \leq x_{i+1} \\ 0 & \text{other conditions} \end{cases} \quad (3-2)$$

$$N_{i,k}(t) = \frac{(t - x_i)}{(x_{i+k-1} - x_i)} N_{i,k-1}(t) + \frac{(x_i - t)}{(x_{i+k} - x_{i+1})} N_{i+1,k-1}(t) \quad (3-3)$$

Hereinto :

Expression $P(t)$ is information point that produces by B-Spline fitting.

Parameter t is a custom variable. In general, it is time or distance. Its maximum value and minimum value happen at the two end points of the curve, generally taking $x_{\min} \leq x < x_{\max}$.

Parameter x_i is knot vector.

Expression $n+1$ is the number of controlling points (characteristic points).

Parameter k is the order of the curve and its degree is $k-1$.

Expression $N_{i,k}(t)$ is the blending function of B-Spline.

Parameter V_i is the position vector of controlling points.

The so-called knot vector must be non-decreasing real number, and the number of the knot vector must be the sum of the number of controlling points $n+1$ and the order of the curve k .

3.1.3 Curve of Non-Uniform Rational B-Spline (NURBS)

B-Spline curve shows its excellent property in the design of curve. The only disadvantage is that it cannot precisely express a section or complete elliptical arc or hyperbola segment. Of course, it follows that it cannot express a section or complete round arc. But a section or complete round is a kind of common curve. Especially in the external design of industrial products, there are many parts that are a section of a complete round curve. Approximate expression with multinomial curve will cause unnecessary design error. If we do not use B-Spline, a new method, which can precisely express senior curve, must be introduced. The new method itself may be not so complex, but it might bring more difficulties in using computers to handle figures. The more applicable method to look for is a kind of curve expression method that can include the existent result as special cases, and also overcome the disadvantage. This method chosen is the curve of Non-uniform Rational B-Spline. NURBS is the abbreviating form of Non-uniform Rational B-Spline, and the specific explanation is as following:

Non-uniform: means that the distance of each knot is variable, therefore, the controlling scope of each controlling peak can be changed.

Rational: means that it allows using weight to each controlling point. Each NURBS object can be expressed by a uniform mathematic expression.

B-Spline: means taking B-Spline as the base function.

A curve of k-order Non-Uniform Rational B-Spline can be defined as the following:

$$P(u) = \frac{\sum_{i=0}^n N_{i,p}(u) \omega_i P_i}{\sum_{i=0}^n N_{i,p}(u) \omega_i} = \sum_{i=0}^n P_i R_{i,p}(u) \quad (3-4)$$

$$R_{i,p}(u) = \frac{\omega_i N_{i,p}(u)}{\sum_{j=0}^n \omega_j N_{j,p}(u)} \quad (3-5)$$

Hereinto: parameter $\omega_i, i = 0, 1, \dots, n$ is called weight factor. It corresponds to its controlling point $P_i, i = 0, 1, \dots, n$. Expression $N_{i,p}(u)$ is the corresponding base function of B-Spline.

The knot vector is $U = [u_0, u_1, \dots, u_m]$, and the number of knot is $m = n + p + 1$.

To NURBS curve, weight factor ω_i only affects the curve shape of the corresponding part of $[u_i, u_{i+p+1}]$. With the change of ω_i , the points $P(u)$ having the same u are on the same straight line (see the Figure 3-1).

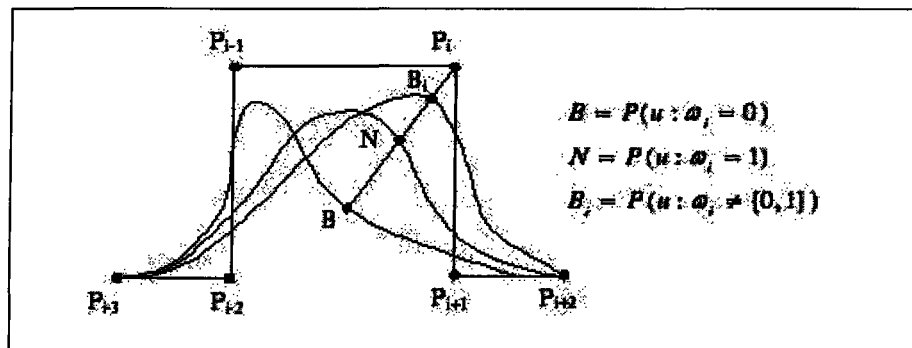


Figure 3-1 the geometric meaning of weight factor

Because when $\omega_i \rightarrow +\infty$, $R_{i,p}(u) = 1$, thus, $P(u)$ is controlling peak P_i ; when $\omega_i = 0$, $R_{i,p}(u) = 0$, and $P(u)$ is the end point B of the straight line. At this time, the controlling peak P_i has no influence on the straight line; when $\omega_i = 1$, $P(u)$ is the point N in the straight line; when $\omega_i \neq 0$ and $\omega_i \neq 1$, $P(u)$ is the point B_i in the straight line. The calculation formula of $R_{i,p}(u)$ in the formula (3-5) changes into the formula (3-6) when all peaks and weight factors except ω_i do not change. The cross ratio calculated from formula (3-7) equals to ω_i .

$$\left\{ \begin{array}{l} \alpha = R_{i,p}(u) = \frac{N_{i,p}(u)}{\sum_{i \neq j=0}^n \omega_j N_{j,p}(u) + N_{i,p}(u)} \quad (\omega_i = 1) \\ \beta = R_{i,p}(u) = \frac{\omega_i N_{i,p}(u)}{\sum_{i \neq j=0}^n \omega_j N_{j,p}(u) + N_{i,p}(u)} \quad (\omega_i \neq 0,1) \end{array} \right. \quad (3-6)$$

Then the cross-ratio of the four points (P_i, B_i, N, B) is as following:

$$\frac{1-\alpha}{\alpha} : \frac{1-\beta}{\beta} = \frac{\sum_{i \neq j=0}^n \omega_j N_{j,p}(u)}{N_{j,p}(u)} : \frac{\sum_{i \neq j=0}^n \omega_j N_{j,p}(u)}{\omega_j N_{j,p}(u)} = \omega_i \quad (3-7)$$

From these we can know the geometric meaning of ω_i : ω_i equals to the cross-ratio of the corresponding four points P_i, B_i, N, B and ω_i when it takes the value $+\infty, 0, 1$. The four points be produced when $\omega_i \neq 0, 1$. When ω_i augments, B_i comes close to P_i , when ω_i reduces, B_i is apart from P_i .

3.1.4 Surface of Non-Uniform Rational B-Spline

The NURBS surface defined by double parameter variable subsection rational multinomial is as following^[12]:

$$\begin{aligned}
 P(u, v) &= \frac{\sum_{i=0}^m \sum_{j=0}^n N_{i,p}(u) N_{j,q}(v) \omega_{i,j} P_{i,j}}{\sum_{i=0}^m \sum_{j=0}^n N_{i,p}(u) N_{j,q}(v) \omega_{i,j}} \\
 &= \sum_{i=0}^m \sum_{j=0}^n P_{i,j} R_{i,p;j,q}(u, v) \quad (u, v) \in [0,1] \quad (3-8)
 \end{aligned}$$

Hereinto: expression $N_{i,p}(u)$ and $N_{j,q}(v)$ are the base functions of B-Spline along u direction and v direction. Parameter $P_{i,j}$ is the line of characteristic controlling points in the rectangle domain. Parameter $\omega_{i,j}$ is the weight factor of the corresponding controlling point. It regulates that the weight factor of the four angles should be positive weight factor, i.e. $\omega_{0,0}, \omega_{m,0}, \omega_{0,n}, \omega_{m,n} > 0$, and the rest $\omega_{i,j} \geq 0$. Expression of $R_{i,p;j,q}(u, v)$ is double variable rational base function:

$$R_{i,p;j,q}(u, v) = \frac{N_{i,p}(u) N_{j,q}(v) \omega_{i,j}}{\sum_{r=0}^m \sum_{s=0}^n N_{r,p}(u) N_{s,q}(v) \omega_{r,s}} \quad (3-9)$$

The knot vector of the u direction and v direction is respectively:

$$U = [0 = u_0 = u_1 = \dots = u_p, u_{p+1}, \dots, u_{r-p-1}, u_{r-p}, u_{r-p+1} = \dots = u_r = 1] \quad (3-10)$$

$$V = [0 = v_0 = v_1 = \dots = v_q, v_{q+1}, \dots, v_{s-q-1}, v_{s-q}, u_{s-q+1} = \dots = v_s = 1] \quad (3-11)$$

In the formula (3-10) and (3-11), the number of the knot vector is $(r+1)$ along u

direction, and $(s+1)$ along v direction. And $r=m+p+1, s=n+q+1$.

3.1.5 NURBS Curve Fitting

The point obtained from our measure apparatus is the model point^[16]. It is not the controlling point of the curve-controlling polygon. Therefore, we use the data that already exist in the curve to get the controlling point. The curve obtained by this method is the interpolation-curve^[3].

Supposing the number of the model point $Q_k, k = 0, 1, \dots, n$ is $n+1$, the curve goes through these model points. The p -degree NURBS curve equation is:

$$P(u) = \sum_{i=0}^n P_i P_{i,p}(u) \quad u \in (0,1) \quad (3-12)$$

Put the parameter \bar{u}_k that corresponding Q_k into the formula (3-12), we get:

$$Q_k = P(\bar{u}_k) = \sum_{i=0}^n p_i R_{i,p}(\bar{u}_k) \quad k = 0, 1, \dots, n \quad (3-13)$$

Describe the formula (3-13) with matrix:

$$\begin{bmatrix} Q_0 \\ Q_1 \\ \vdots \\ Q_n \end{bmatrix} = \begin{bmatrix} R_{0,p}(\bar{u}_0) & R_{1,p}(\bar{u}_0) & \cdots & R_{n,p}(\bar{u}_0) \\ R_{0,p}(\bar{u}_1) & R_{1,p}(\bar{u}_1) & \cdots & R_{n,p}(\bar{u}_1) \\ \vdots & \vdots & \ddots & \vdots \\ R_{0,p}(\bar{u}_n) & R_{1,p}(\bar{u}_n) & \cdots & R_{n,p}(\bar{u}_n) \end{bmatrix} \begin{bmatrix} P_0 \\ P_1 \\ \vdots \\ P_n \end{bmatrix} \quad (3-14)$$

The element of equation (3-14) is value of the base function of B-Spline according \bar{u}_k . If we want to get the vector of controlling points using equation (3-14), we need transform model point to parameter firstly, and then get \bar{u}_k and the knot vector U .

The process of get \bar{u}_k and U is shown as the Figure 3-2.

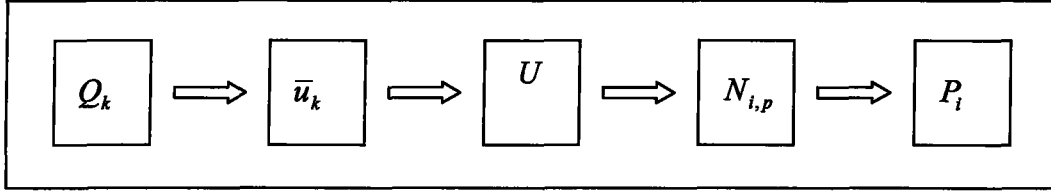


Figure 3-2 the process of the getting parameter of curve

We can use the formula (3-15) to get parameter \bar{u}_k .

$$\bar{u}_0 = 0$$

$$\bar{u}_n = 1$$

$$\bar{u}_k = \bar{u}_{k-1} + \frac{|Q_k - Q_{k-1}|^{\frac{1}{2}}}{\sum_{j=1}^n |Q_j - Q_{j-1}|^{\frac{1}{2}}} \quad k = 1, 2, \dots, n-1 \quad (3-15)$$

We use Average Method to get the U as formula (3-16)

$$u_0 = \dots = u_p = 0$$

$$u_{m-p} = \dots = u_m = 1$$

$$u_{j+p} = \frac{1}{p} \sum_{i=j}^{j+p-1} \bar{u}_i \quad j = 1, \dots, n-p \quad (3-16)$$

Knot vector is:

$$U = \{0 = u_0 = \dots = u_p, u_{j+p}, u_{m-p} = \dots = u_m = 1\}, \quad m = n + p + 1 \quad (3-17)$$

And the base function of B-Spline is:

$$N_{i,0}(u) = \begin{cases} 1 & u_i \leq u \leq u_{i+1} \\ 0 & \text{else} \end{cases}$$

$$N_{i,p}(u) = \frac{u - u_i}{u_{i+p} - u_i} N_{i,p-1}(u) + \frac{u_{i+p+1} - u}{u_{i+p+1} - u_{i+1}} N_{i+1,p-1}(u) \quad (3-18)$$

Now, the model point Q_k , parameter \bar{u}_k , knot vector $U = [u_0, u_1, \dots, u_m]$ and the base function of B-Spline have been obtained. Based on the formula (3-14) we can obtain the controlling point $P_i, i = 0, 1, \dots, n$ using Gauss Elimination Method, and then produce an interpolation curve.

3.1.6 NURBS Surface Fitting

In this part, we use interpolation to fit the free surface by NURBS surface. The interpolating process of NURBS surface is, according to the given model points shown with the topology matrix array, using the method of interpolation ^[44], to structure a mathematic model. It can so expressed so as to find a group of linear equations of the unknown controlling peak $P_{i,j}, i = 0, 1, \dots, m; j = 0, 1, \dots, n$, but this group of linear equations is often so huge that it can be difficult to solve ^[46]. The algorithm used in this thesis is the reverse process. Transform the problem into two process of curve reverse. The process is:

1) Parameter direction and parameter choice

To data point matrix $Q_{i,j}, i = 0, 1, \dots, m; j = 0, 1, \dots, n$, supposing i^{th} ($i = 0, 1, \dots, m$) row data point $Q_{i,j}, j = 0, 1, \dots, n$ is plane data point. There are $m + 1$ planes, taking u as parameter. The column direction is the vertical parameter direction, taking v as parameter.

2) Determining Knot Vector

To make the data point $Q_{i,j}, j = 0, 1, \dots, n$ of the i^{th} row of u direction to become parameter; we can use the method of Centripetal Parameter. Supposing parameter is $u_{i,j}, j = 0, 1, \dots, n$:

$$u_{0,j} = 0$$

$$u_{m,j} = 1$$

$$u_{i,j} = u_{i-1,j} + \frac{|Q_{i,j} - Q_{i-1,j}|^{\frac{1}{2}}}{\sum_{i=1}^m |Q_{i,j} - Q_{i-1,j}|^{\frac{1}{2}}} \quad i = 1, \dots, m-1 \quad (3-19)$$

The public u direction is:

$$u_0 = 0$$

$$u_m = 1$$

$$u_i = \frac{1}{m+1} \sum_{j=0}^m u_{i,j} \quad i = 1, \dots, m-1 \quad (3-20)$$

Similarly, the public v direction is:

$$v_0 = 0$$

$$v_n = 1$$

$$v_j = \frac{1}{n+1} \sum_{i=0}^n v_{i,j} \quad j = 1, \dots, n-1 \quad (3-21)$$

In this way, the knot vectors U and V of the direction of the two parameters can be determined.

3) Finding the base functions $N_{i,p}, N_{j,q}$ of NURBS.

$$N_{i,0}(u) = \begin{cases} 1 & u_i \leq u \leq u_{i+1} \\ 0 & \text{else} \end{cases}$$

$$N_{i,p}(u) = \frac{u - u_i}{u_{i+p} - u_i} N_{i,p-1}(u) + \frac{u_{i+p+1} - u}{u_{i+p+1} - u_{i+1}} N_{i+1,p-1}(u) \quad (3-22)$$

Similarly, the $N_{j,q}$ can be obtained.

4) Counting reversely the controlling peak.

In the knot vector U , the degree is p , for the data points in the i^{th} row ($i = 0, \dots, m$), making use of curve reverse counting constructs section line of the i^{th} row, and finds the controlling point $D_{i,j}, j = 0, \dots, n$. Do not change parameter j , and in the knot vector V , the degree is q ; calculate the controlling peak $D_{i,j}, j = 0, \dots, n$ in the j^{th} column ($j = 0, \dots, n$) as “data point”, and then uses reverse counting and finds the controlling peak $P_{i,j}$ in the j^{th} column. And $P_{i,j}, i = 0, \dots, m; j = 0, \dots, n$ is the controlling peak of the surface that we want to calculate. Together with knot vectors U, V , a NURBS surface with the degree $p \times q$ is determined.

3.2 Noise Point of Right and Left CCD Filtering

If use is made of a single CCD structure for our measurements, the speed is very fast. But, a single CCD cannot get the profile information in many places of objects, because when the CCD is in one side, the measured point is in the other side of the object and there are some higher points preventing the beam. In order to solve the problems above,

we use a double CCD measuring system. But another problem appears with it, that is, in the process of scanning, the information gathered from a double CCD has a coincident part. Therefore, we should handle the information of these two parts.

In the process of characteristic point data fitting of right and left CCD, it is enough to handle the measurement with not as high a requirement for precision if the method of filtering the noise points is not used. But if the filter process is added into the process of data fitting, the precision will further increase. So in the following I will introduce the method of filtering noise points originated in this thesis.

First, according to the precision requirement of measurement and the sampling length of characteristic points, select a scale.

Then, based on this scale, analyze the characteristic points of the right and left CCD respectively. First, compare each point of the left CCD with all points of the right CCD, if all distances between the first point of the left CCD and all points of the right CCD are more than the selected scale, then this point should be deleted; then compare the second point of the left CCD with all points of the right CCD, followed by the rest of the points of the left CCD compared with the same method.

After the points of the left CCD are all compared Reverse the process, compare the points of the right CCD with each point of the left CCD. So, the noise points in the right CCD can be filtered.

Finally, through the rest characteristic points, with the method of fitting the final result will be got.

The figures of 3-3 and 3-4 are the final error analysis results obtained through the method without noise point filtering and with noise point filtering to the standard sphere. From the results, we can see that if the scale is selected properly, the measuring precision will be increased.

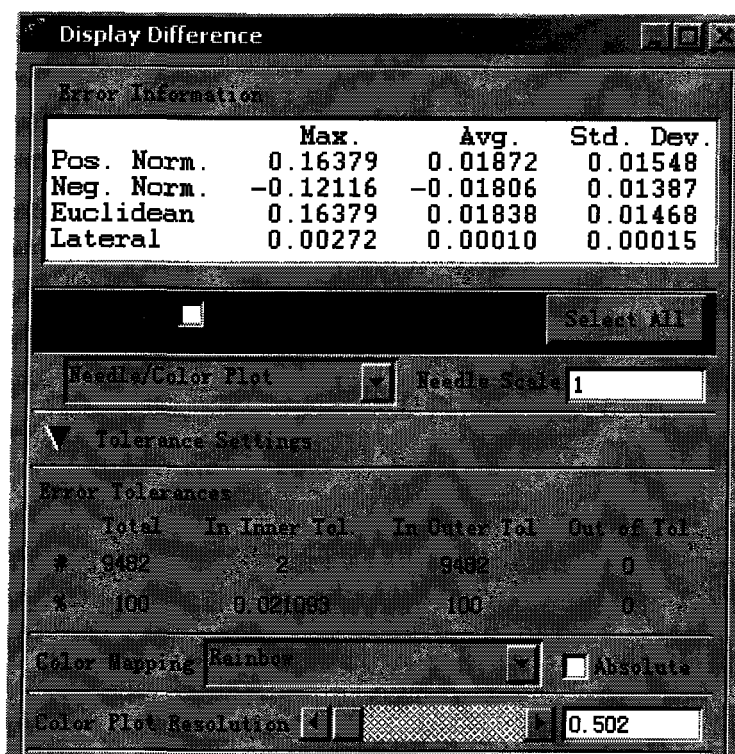


Figure 3-3 the error result got through the method without noise point filtering

CHAPTER 4

THE CALCULATION OF SURFACE ERROR

In this chapter we deal with the problem of calculating the form error. In the industrial context, machines produce products according some derived CAD model. We call this appointed CAD model the standard surface. The produced products are generally the same as the CAD model. But during the production, due to reasons of data handling, equipments, and operation and so on, there may be some error. What we want to do is to find and calculate the form error of the products, and then according to the scale of the acceptable form error to judge whether the products are qualified.

Now, the methods of measuring form error are mostly used to measure simple geometric form^[48]. There is not so much research of the form error of complex geometric form. It brings intricate problems and constrains technology development. With the rapid development of aviation, spaceflight, shipbuilding, automobile and mould industry, the measuring requirements of efficiency and precision are more critical. The shape of free surface is very complex, and its measuring method, at present the most universal, is Coordinates Method represented by three-dimensional measuring machines. Although

there are some researchers putting forward some novel methods for the form error of complex surface^[4], based on the Least Region Method, the mathematic model to calculate the form error is still very complex^[1]. Up to now, the calculation of the form error of the complex surface according to the Least Region Method is still a difficult problem. But the Genetic Algorithm has an advantage in handling this kind of complex non-linear optimizing problem, and this algorithm is easy to be implemented on a computer. The traditional Genetic Algorithm uses binary system encoding. Although the operation is simple, to the optimization of real number space, the contradiction among calculation precision and encoding length and calculation workload still exists. Therefore, this thesis puts forward the Genetic Algorithm of real number encoding as a viable approach.

4.1 Assessing Method of Surface Form Error

In the previous chapter, we get the fitting surface through the data points of the measured object, and now we need to calculate the form error between measured surface and the standard surface. The method of assessing form error is the Least Region Method.

4.1.1 Definition of Surface Form Error

As figure 4-1 shows, we approach the surface got in the actual measurement with two standard surfaces. It makes the measured surface to be contained into two standard surfaces. When the distance between the two standard surfaces is the smallest, the distance

is the form error value we want to calculate ^[29]. This method is called the Least Region Method. The Least Region Method is the best method of assessing curve and surface form error ^[19].

According to the Least Region Method to assess the form error of the complex surface, the error value is the smallest distance of the two standard surfaces when the two standard surfaces just contain the measured surface ^[21].

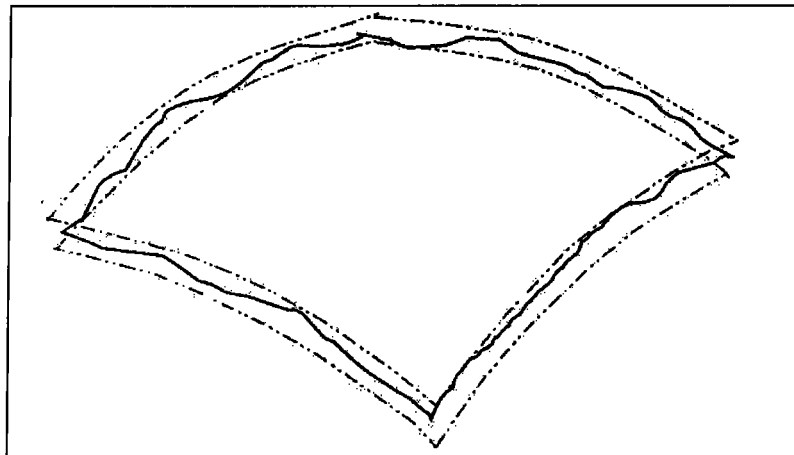


Figure 4-1 the definition of surface form error ^[42]

4.1.2 Transformation of 3D Coordinates of the Measured Point

A parameter surface has geometric invariability and mapping invariability. The so-called geometric invariability means that the parameter surface has the invariable property of shape not relying on the choice of coordinate system or the coordinates rotation

and translation. In order to make the theoretic design surface (standard surface) and the actual measured point be the best matching state, the measured point must be translated, rotated and coordinates transformation. Supposing the coordinates of the measured point is:

$$P = \{P_j = (x_j^R, y_j^R, z_j^R) \mid j = 1, 2, \dots, m\} \quad (4-1)$$

The original position of the theoretic design surface is (x_0, y_0, z_0) . According to the transformation relation, the matrix of coordinates' transformation moving the original measured point near the origin is as the following:

$$T_p = \begin{bmatrix} 1 & 0 & 0 & 0 \\ 0 & 1 & 0 & 0 \\ 0 & 0 & 1 & 0 \\ -x_1^R + \Delta x & -y_1^R + \Delta y & -z_1^R + \Delta z & 1 \end{bmatrix} \quad (4-2)$$

In the formula: $\Delta x \in [-\lambda l, \lambda l]$;

$$\Delta y \in [-\lambda l, \lambda l];$$

$$\Delta z \in [-\lambda l, \lambda l];$$

$$l = \max \{ \max \{x_j \mid j = 1, 2, \dots, m\} - \min \{x_j \mid j = 1, 2, \dots, m\}, \\ \max \{y_j \mid j = 1, 2, \dots, m\} - \min \{y_j \mid j = 1, 2, \dots, m\}, \\ \max \{z_j \mid j = 1, 2, \dots, m\} - \min \{z_j \mid j = 1, 2, \dots, m\} \}$$

Parameter λ is constants and can take the value 0.01~0.1 according to the specific condition.

After the measured point is translated and rotated along the x -axis, y - axis, and z -axis, its transformation matrix is as the following:

$$T = T_p T_x T_y T_z \quad (4-3)$$

In the formula, T_x is the transformation matrix of the measured point rotating along x -axis, and the value scope of its angle θ is $\theta \in [\theta_0, \theta_1]$; T_y is the transformation matrix of the measured point rotating along y -axis, and the value scope of its angle ϕ is $\phi \in [\phi_0, \phi_1]$; T_z is the transformation matrix of the measured point rotating along z -axis, and the value scope of its angle ψ is $\psi \in [\psi_0, \psi_1]$.

The new coordinates after the measured point transformation are:

$$[x_j^*, y_j^*, z_j^*, 1] = [x_j^R, y_j^R, z_j^R, 1]^T \quad (4-4)$$

4.1.3 Calculation of the Smallest Distance from the Measured Point to the Standard Surface

Supposing the parameter equation of the standard surface is as the following:

$$\begin{cases} x = x(u, v) \\ y = y(u, v) \\ z = z(u, v) \end{cases} \quad (4-5)$$

In the formula: $u \in [u_b, u_e]$; $v \in [v_b, v_e]$.

Then the distance from the measured point to a point of the standard surface is dt_j :

$$dt_j = \sqrt{[x_j^R - x(u, v)]^2 + [y_j^R - y(u, v)]^2 + [z_j^R - z(u, v)]^2} \quad (4-6)$$

Then the smallest distance from the measured point to the standard surface is as the following:

$$dt_{j\min} = \min(\sqrt{[x_j^R - x(u, v)]^2 + [y_j^R - y(u, v)]^2 + [z_j^R - z(u, v)]^2}) \quad (4-7)$$

Obviously, calculating the smallest distance from the measured point to the standard surface itself is an optimizing problem. It can distribute $m_u \times m_v$ points symmetrically on the standard surface along the direction of the parameters u, v , i.e.:

$$P = \{P_{i,j} = (u_i, v_j) \mid i = 1, 2, \dots, m_u; j = 1, 2, \dots, m_v\} \quad (4-8)$$

In the formula: The value of m_u, m_v can be selected according to the degree of complexity of the standard surface.

And then it should solve respectively the distance from some measured point to these points and find the point that corresponding the smallest distance in the surface. And then, find the corresponding parameters u_{N1}, v_{N2} of the point that we find just now. The general position of foot of perpendicular corresponding to the smallest distance from the measured point to the standard surface lies in the following region.

$$\begin{aligned} u &\in \left[u_{N1} - \frac{u_b - u_e}{m_u}, u_{N1} + \frac{u_b - u_e}{m_u} \right], \\ v &\in \left[v_{N2} - \frac{v_b - v_e}{m_v}, v_{N2} + \frac{v_b - v_e}{m_v} \right] \end{aligned} \quad (4-9)$$

After the handling mentioned above, it is possible to use the method of the traditional multiple function optimizing to make precise calculation.

4.2 Form Error Calculation of the Complex Surface Based on Genetic Algorithm

4.2.1 Establishment of the Mathematic Model of the Form Error

In the process of Computer Assisting Design and Computer Assisting Manufacture (CAD/CAM), the external profiles of some objects are the regular surfaces that can be described by the known mathematic model like sphere, ellipse, and hyperbola surface. But in industrial production, the most of surfaces are the free surfaces.

When measuring the form error we need to get the mathematic model of the standard surface ^[17]. Only by this can we calculate the distance from the point to the standard surface.

The parameter equation of the mathematic model of the regular standard surface is as following:

$$\begin{cases} x = x(u, v) \\ y = y(u, v) \\ z = z(u, v) \end{cases} \quad (4-10)$$

In the formula: $u \in [u_b, u_e]; v \in [v_b, v_e]$.

The mathematic model of the free standard surface with complex anomalistic shape is expressed by a group of discrete points' coordinates, but the mathematic model is unknown. In the production, these discrete points can produce the products. Therefore, to find the mathematic model of the free standard surface are needed in calculating the form

error, it needs to fit this standard surface using these discrete points. Similarly, we also use NURBS fitting method to fit the free standard surface and the specific method has been introduced in chapter three. After we have the mathematic model of the free standard surface, we can combine the Least Region Method to calculate the form error of the surface.

Only when the position of the standard surface is optimal, can it guarantee that the distance among the standard surface containing all the measured points is the smallest. Therefore, it is a very complex non-linear optimizing problem. To finish this process, the following steps are needed:

- 1) Moving the original point of the standard surface to the coordinate origin.
- 2) Moving the measured point near the coordinate origin.
- 3) Rotating the measured surface along x -axis, y -axis, and z -axis.
- 4) After coordinates' transformation, calculate the smallest distance from the measured point to the standard surface.

Because foot of perpendicular of each measured point may fall in different NURBS surface section of the standard surface, it must divide different NURBS surface section and use the method introduced before to solve the smallest distance e_i from the measured point to the standard surface.

- 5) Find the maximum of the smallest distance from all the measured points to the standard

surface, i.e.:

$$e_{\max} = \max\{e_j \mid j = 1, 2, \dots, m\} \quad (4-11)$$

After moving standard surface to the origin, and moving the measured point of the measured surface near the origin, and rotating along x -axis, y -axis, and z -axis, the direct distance of standard surfaces containing all the measured points, in essence, is twice of the maximum of the distance e_j from each measured points to the standard surface, i.e.:

$$r = 2e_{\max} \quad (4-12)$$

Only when the positions of the measured surface and the standard surface are optimal, can it guarantee that the direct distance of the standard surfaces containing all the measured points is the smallest, that is, it satisfies the assessing standard of the Least Region Method. This is a very complex non-linear optimizing problem that can be well solved using the Genetic Algorithm of real number encoding.

4.2.2 Genetic Algorithm of Real Number Encoding

4.2.2.1 Genetic Algorithm

Since life first originated on the earth, in order to adapt to the environment, life began a long evolutionary process. In 1859, Darwin, the British biologist put forward the theory of The Origin of Species that is now famous throughout the world. In this work, he put forward the theory of biology evolution based on natural selection. This theory states

that the evolution of biological species arises from three kinds of factors: heredity, aberrance and selection. The biology evolves from the lower level to the higher level continuously in the comprehensive process of heredity and aberrance. And selection works through heredity and aberrance. Aberrance provides new genes for selection. Heredity strengthens and keeps the selected genes. Selection can control the direction of heredity and aberrance to make them develop forward the direction of adapting the environment.

The biology theory put forward by Darwin exposed the evolutionary process of the natural world. This process edifies the scientists. There hides a kind of advanced notion of searching and optimizing in the process of natural selection. The scientists look for new inspiration used in artificial system through the evolutionary process of the biology. In the middle of the 1950s, they founded the Bionics and developed the Imitating Evolutionary Algorithm. The algorithm is suitable for the optimizing problem in the actual world. This work, combines life science and computing science, make the life science become a constituent of computing science. Among them, the Genetic Algorithm put forward by Holland ^[20] has made great achievements.

The Genetic Algorithm is a kind of structural random search. It imitates the process of biology evolution. When solving the given optimization task, the algorithm begins to collect several estimated parameters (called Chromosome). Each parameter is estimated by its adaptation degree function. In each generation, the chromosome with high adaptation

degree is allowed to cross-match and to reproduce. The produced new estimated parameters form the basis of the next generation. This biology imitating process will give an effective solution to the complex problem. The GA (Genetic Algorithm) was first put forward by Holland, and was broadly develop by Goldberg ^[18].

Genetic Algorithm has been successfully applied in many kinds of optimizing problems ^[15], the parameter estimation of linear self-adapted filter ^[14] and parameter identification of non-linear figure filter ^[51], static data relevancy of multi-sensor and multi-target ^[39], and so on. Meanwhile, the Genetic Algorithm has gone into many disciplines and fields, such as genetic programming, machine learning and artificial intelligence, and so on.

4.2.2.2 Genetic Algorithm of Real Number Encoding

The traditional Genetic Algorithm uses binary system encoding whose characteristic is easy genetic operation. But there are some disadvantages in finding optimization of real number space as following:

- Binary system encoding makes the continuous space discrete by people. It causes the contradiction among the precision calculating, encoding length, and calculating workload.
- Because of the constraint of the encoding, it is possible to approach the optimized solution, but it is not the actual optimized solution.

To solve the problem mentioned above and enlarge the scope of optimization problems, it becomes relevant to use real number encoding. The strategy of real number encoding with high precision and convenient has been paid more and more attention to. Some researchers put forward different strategies of real number encoding and the genetic operation. But the Genetic Algorithm based on real number encoding generally uses arithmetic genetic operator but not gene genetic operator. It is hard to analyze its performance. Therefore, this thesis puts forward an improved real number encoding and uses the genetic operator and the analyzing method of binary system encoding. We called it as unitary real number encoding. Then we get the genetic operator of unitary real number encoding and similar mode rule.

1) The definition of the unitary real number encoding

According to the basic definition of the Genetic Algorithm of binary system encoding, the definition of the unitary real number encoding is given in this thesis.

The general form of the optimizing problem is as the following:

$$\min f(x), \quad x = (x_1, x_2, \dots, x_n) \quad (4-13)$$

The feasible region of the solution of any complex finding optimization problem in continuous space can be mapped into the scope of $[0, 1]$.

The value range of the unitary real number encoding is $(0, 1)$. It evolves from the binary system encoding. And its gene unit is decimal unit with the ten possible values from

0 to 9.

Identical to the controlling parameter of the standard Genetic Algorithm, the controlling parameters of the Genetic Algorithm of the unitary real number encoding mainly include the population size n , the selection probability p_s , cross probability p_c and the variation probability p_m , and so on. The selection of these parameters directly affects the performance of the Genetic Algorithm. Therefore, how to select these controlling parameters is still the concerned problem.

2) The mode of unitary real number encoding

The mode is a template describing the set of the character string.

To unitary real number encoding, the character set is $\{0,1,2,3,4,5,6,7,8,9\}$. From this, the set of the character string of decimal fraction can be produced. If adding a wildcard character "*", then the character set enlarges into $\{0,1,2,3,4,5,6,7,8,9,*\}$, from which the set of the character string like 0.12347, 0.2*4*5, 0.**5*0, and so on, can be produced.

The set of the character string with similar structure produced based on eleven character set $\{0,1,2,3,4,5,6,7,8,9,*\}$ is called the mode of unitary real number encoding.

3) Determining the encoding length of unitary real number encoding

The encoding length is one of the important parameters affecting the performance of the Genetic Algorithm of unitary real number encoding.

➤ The determining of the encoding length of the one-dimensional real number encoding.

Supposing the calculating precision of the optimizing problem is $\varepsilon = 10^{-m}$, and the practicable region of the one-dimensional optimizing problem is $x \in [x_1, x_2]$, we can get:

$$x_{\max} = \max\{|x_1|, |x_2|\} \quad (4-14)$$

The encoding length of the one-dimensional real number encoding is:

$$L \geq \text{int}(\lg x_{\max}) + 1 + m \quad (4-15)$$

Hereinto, equation $\text{int}()$ means taking the integer. From the formula (4-15), it can be seen that the encoding length of unitary real number encoding has some relations with the decimal of the calculating precision and the largest absolute value of the border of the definition region. The formula (4-15) provides theoretic foundation for determining the encoding length of unitary real number encoding of the one-dimensional optimizing problem.

➤ The determining of the encoding length of the multi-dimensional real number encoding.

Supposing the calculating precision of the optimizing problem is $\varepsilon = 10^{-m}$, each component of the practicable region of the multi-dimensional optimizing problem is:

$$x_i \in [x_{i,1}, x_{i,2}], i = 1, 2, \dots, k \quad (4-16)$$

Then the encoding length of the multi-dimensional real number encoding is:

$$L \geq \text{int}(\lg x_{\max}) + 1 + m \quad (4-17)$$

From the formula (4-17), it can be seen that the encoding length of unitary real number encoding has some relations with the decimal of the calculating precision and the largest absolute value of the border of the definition region. The formula (4-17) provides theoretic foundation for determining the encoding length of unitary real number encoding of the multi-dimensional optimizing problem.

4) Determining the population size of unitary real number encoding

Supposing population size of the Genetic Algorithm of unitary real number encoding is n , the genetic operation can produce n^{10} modes. Obviously, the larger the n is, the smaller the possibility that the algorithm gets into the part optimizing solution will be. If it is like this, it can effectively restrain the problem of pre-maturity. But too large population size will increase the calculating workload and will affect the calculating efficiency. Therefore, the selecting of the population size has great influence on the performance of the Genetic Algorithm.

If the encoding length of one individual is L , and the number of elements in its set of the character string is G , then there are $(G+1)^L$ different models in one individual. In the population, the more the number of the models that can at least match one individual is, the richer the diversity of the population will be. If all the new individuals are produced randomly, then the population size of binary system encoding is:

$$n = (2)^{L/2} \quad (4-18)$$

The population size of real number encoding is:

$$n = (10)^{L/10} \quad (4-19)$$

In order to guarantee the diversity of the population, for the same encoding length, the population size of the binary system encoding is larger than that of unitary real number encoding, which means that to the same population size, the diversity of unitary real number encoding is higher than that of the binary system encoding. In the Genetic Algorithm of the binary system encoding actually used, the general population size n is 10~160, while the general population size of the Genetic Algorithm of unitary real number encoding is 10~100.

5) The Cross Operator of the Genetic Algorithm of real number encoding

The effectiveness of the Genetic Algorithm mainly comes from selection and cross. Especially the cross arithmetic operator, it is the main method of mode generation and plays the important role.

The cross arithmetic operators often used include: one-point cross, two-points cross, multi-points cross, heuristic cross, sequence cross and mixed cross, and so on. Among them, the one-point cross is used more often. Take the one-point cross for example to illustrate the operation of cross operator of the unitary real number encoding.

The one-point cross is that, randomly setting intersection from the two individuals.

Exchange the structure of the two individuals after intersection. Thereby, two new individuals come into being as is shown in the Figure 4-2. In the Figure 4-2, the intersection is between the third gene unit and the fourth unit. After the cross operation, the gene units' positions after this intersection are interchanged. Thereby, the two individual A' and B' are produced. Because the intersection is random, when the length of character string of the individual is L , there will be $(L-1)$ possible intersections. Therefore one-point cross can get $(L-1)$ possible results.

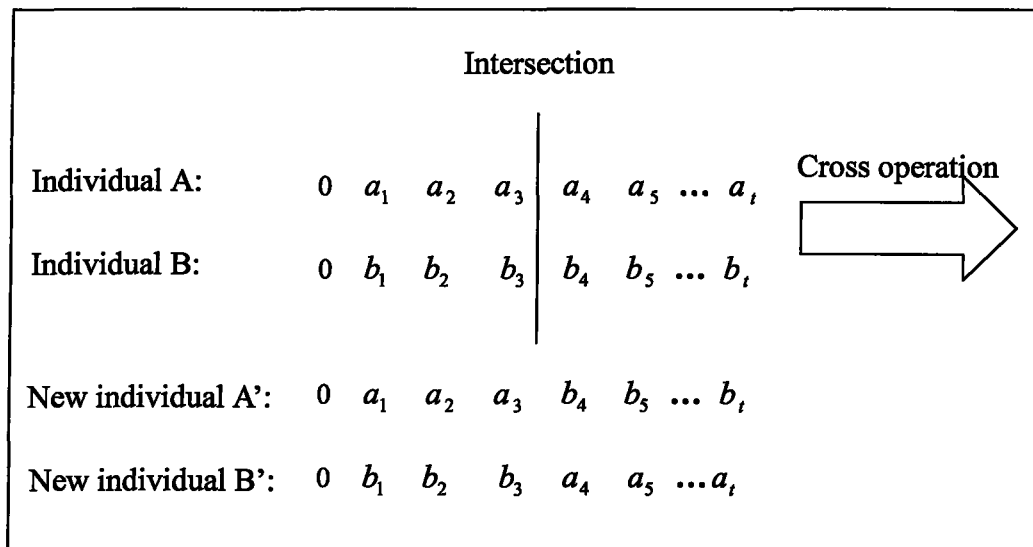


Figure 4-2 the cross operation of the unitary real number encoding

6) Variation operation of the Genetic Algorithm of unitary real number encoding

To the Genetic Algorithm of the unitary real number encoding, because it is the

encoding based on the character set of $\{0,1,2,3,4,5,6,7,8,9\}$, its variation operation is not so easy as the Genetic Algorithm of the binary system. The basic process is as following:

- In the population, according to the variation probability p_m , randomly select individual.
- In the selected individual whose length of character string is L , randomly decide variation gene unit. And then in the other nine characters except the current gene unit value in the character set of $\{0,1,2,3,4,5,6,7,8,9\}$, randomly select a value replacing original value of gene unit. Therefore, there are nine different possibilities of gene variation value.

7) The adaptation degree function of the Genetic Algorithm of unitary real number encoding

In the Genetic Algorithm, the adaptation degree is the ruler. It can assess the quality of the individuals in population. The larger the adaptation degree of the individual is, the more excellent the individual is; otherwise, the smaller the adaptation degree of the individual is, the less excellent the individual is. In the process of evolutionary search, the Genetic Algorithm is only need the adaptation degree function, needing no pre-condition or the other information. So the dependence on the problem itself is small.

The adaptation degree function is non-negative. But in many optimizing problems, the objective function is the minimum of cost function, not the maximum of the advantage function. So, some problems are expressed in the form of solving the maximum, it cannot

guarantee that the advantage function takes the non-negative value for all the variables. Therefore, to these problems, it is common to transform the objective function into the adaptation degree function.

When the objective function is the advantage function, in order to guarantee the adaptation degree function is non-negative, its adaptation degree function is:

$$fit(x_i^t) = f_1(x_i^t) - C_{\min} \quad (4-20)$$

Hereinto, parameter C_{\min} is the minimum of the advantage function of the individual in the up-to-date population.

When the objective function is the cost function, its adaptation degree function is:

$$fit(x_i^t) = C_{\max} - f_2(x_i^t) \quad (4-21)$$

Hereinto, parameter C_{\max} is the maximum of the cost function of the individual in the up-to-date population.

4.2.3 Calculation of the Surface Form Error

From the mathematic model of the form error of the complex surface, it is known that the form error value is determined by the six parameters $(\Delta x, \Delta y, \Delta z, \theta, \phi, \psi)$. Therefore, when using the Genetic Algorithm to calculate the form error of the complex surface, parameters $(\Delta x, \Delta y, \Delta z, \theta, \phi, \psi)$ are needed to have unitary encoding, i.e. $(\Delta x_s, \Delta y_s, \Delta z_s, \theta_s, \phi_s, \psi_s)$. The region of θ, ϕ, ψ is:

$$\begin{cases} 0 \leq \theta \leq 2\pi \\ 0 \leq \phi \leq 2\pi \\ 0 \leq \psi \leq 2\pi \end{cases} \quad (4-22)$$

The encoding of $(\Delta x, \Delta y, \Delta z, \theta, \phi, \psi)$ using unitary encoding is:

$$0 \leq \Delta x_s \leq 1; 0 \leq \Delta y_s \leq 1; 0 \leq \Delta z_s \leq 1;$$

$$0 \leq \Delta \theta_s \leq 1; 0 \leq \Delta \phi_s \leq 1; 0 \leq \Delta \psi_s \leq 1;$$

The mapping relationship between $(\Delta x, \Delta y, \Delta z, \theta, \phi, \psi)$ and $(\Delta x_s, \Delta y_s, \Delta z_s, \theta_s, \phi_s, \psi_s)$ is:

$$\Delta x = (2\Delta x_s - 1)\lambda l$$

$$\Delta y = (2\Delta y_s - 1)\lambda l$$

$$\Delta z = (2\Delta z_s - 1)\lambda l$$

$$\theta = 2 \cdot \pi \cdot \theta_s$$

$$\phi = 2 \cdot \pi \cdot \phi_s$$

$$\psi = 2 \cdot \pi \cdot \psi_s$$

Before calculating, firstly, initialization of algorithm is needed. The steps of process are:

- 1) Selecting the controlling parameter

The controlling parameter of the Genetic Algorithm is usually selected according to experiments. According to the form error of the complex surface and through large number of experiments, the more satisfied controlling parameter is: population size $n = 50$; the cross

probability $p_c = 0.8$; the variation probability $p_m = 0.02$; the maximum of evolution generation $t_{\max} = 1000$.

2) Determining the encoding length of $(\Delta x_s, \Delta y_s, \Delta z_s, \theta_s, \phi_s, \psi_s)$

Supposing the precision is $\varepsilon = 10^{-k}$, the largest absolute value of the feasible region of each variation is the following:

$$dat_{\max} = \max\{\lambda l, 2\pi\} \quad (4-23)$$

The encoding length of each component can be calculated by the following formula:

$$l \geq \text{int}(\lg dat_{\max}) + 1 + k \quad (4-24)$$

3) Determining the initial population

We use the random generator to get random encoding in the feasible region ($0 \leq \Delta x_s \leq 1, 0 \leq \Delta y_s \leq 1, 0 \leq \Delta z_s \leq 1, 0 \leq \Delta \theta_s \leq 1, 0 \leq \Delta \phi_s \leq 1, 0 \leq \Delta \psi_s \leq 1$) and produce the initial population ($t = 0$), i.e.:

$$D(0) = \{(\Delta x_{s,i}^0, \Delta y_{s,i}^0, \Delta z_{s,i}^0, \theta_{s,i}^0, \phi_{s,i}^0, \psi_{s,i}^0) \mid i = 1, 2, \dots, n\} \quad (4-25)$$

4) Determining the adaptation degree function

The objective function of the form error of the complex surface is the maximum of the smallest distance from the each measured point to the standard surface.

$$g(\Delta x_{s,i}^t, \Delta y_{s,i}^t, \Delta z_{s,i}^t, \theta_{s,i}^t, \phi_{s,i}^t, \psi_{s,i}^t) = \max\{e_i^t\}, i = 1, 2, \dots, n \quad (4-26)$$

In the formula, parameter e_i^t is the smallest distance from all measured points

$P = \{(x_j^R, y_j^R, z_j^R) | j = 1, 2, \dots, m\}$ transformed by $(\Delta x_{s,i}^t, \Delta y_{s,i}^t, \Delta z_{s,i}^t, \theta_{s,i}^t, \phi_{s,i}^t, \psi_{s,i}^t)$ to the standard surface.

The value changing of the objective function is reverse to that of the adaptation degree function, that is, the smaller the objective function value is, the bigger the adaptation degree of the corresponding individual will be. Therefore, it needs to establish the mapping relationship between objective function and the adaptation degree function.

$$\begin{aligned} & f(\Delta x_{s,i}^t, \Delta y_{s,i}^t, \Delta z_{s,i}^t, \theta_{s,i}^t, \phi_{s,i}^t, \psi_{s,i}^t) \\ & = g_{\max}^t - g(\Delta x_{s,i}^t, \Delta y_{s,i}^t, \Delta z_{s,i}^t, \theta_{s,i}^t, \phi_{s,i}^t, \psi_{s,i}^t) \end{aligned} \quad (4-27)$$

In the formula: parameter g_{\max}^t is the largest value of the corresponding objective function of the up-to-date population.

5) Selection of operators

We choose the parallel sub-cross operator and parallel sub-variation operator.

In order to guarantee the overall convergence, it preserve the optimizing individual to the filial generation.

4.3 Summary

According to the Least Region Method to assess the form error of complex surface, in essence, it is a very complex non-linear optimizing problem. It is hard to calculate with the traditional method. Therefore, the form error calculation of the complex surface based on the Least Region Method is an unsolved problem. Because the Genetic Algorithm has

the characteristic of solving the complex non-linear optimization, this chapter calculates form error of the complex surface with the method of the Genetic Algorithm of unitary real number encoding, which helps this problem. Through the analysis of the experiment result, the method used in this chapter is completely effective.

CHAPTER 5

PROGRAM DESIGN AND DATA ANALYSIS

5.1 Program Design

The aim of this project is to design a set of complete automatic testing system. The whole process from the measurement of the measured object to judge whether the measured object is qualified can be finished automatically through 3D scanner and computer, and need not transform any data form.

The content of this chapter is to realize the theory and the algorithm mentioned in the previous chapters in software. The user interface of the final form error is given. We use VC++6.0^{[31][34]} to compile the program. The specific steps are as following:

(1) Getting the point data

The point data can be got from the 3D laser scanner. These points have already been transformed into point data in 3D space.

(2) The filtering of the right and left CCD noise points

The profile information of many parts of the objects cannot be obtained when using single CCD to measure. In order to solve this problem, we use double CCD to measure.

But when using double CCD, the noise points will appear. In order to increase the precision, we need to filter the noise points.

The method of filtering the noise points has been introduced in the previous chapter. The filtering process of the noise points in the left CCD is shown in Figure 5-1. The filtering process of the noise points in the right CCD can be realized with the same method. Finally, the rest points in double CCD can be used to fit the surface.

(3) The fitting of the surface

Using the point data got in the steps above, we can get the profile surface of the object through NURBS surface fitting. The flow chart is shown in the Figure 5-2.

(4) Calculating the form error

We use the Least Region Method to get the mathematic model of form error. It is the distances between the two standard surfaces that can just contain the measured surface. This distance is the form error we get in the end. And then calculate the form error with the Genetic Algorithm of unitary real number encoding.

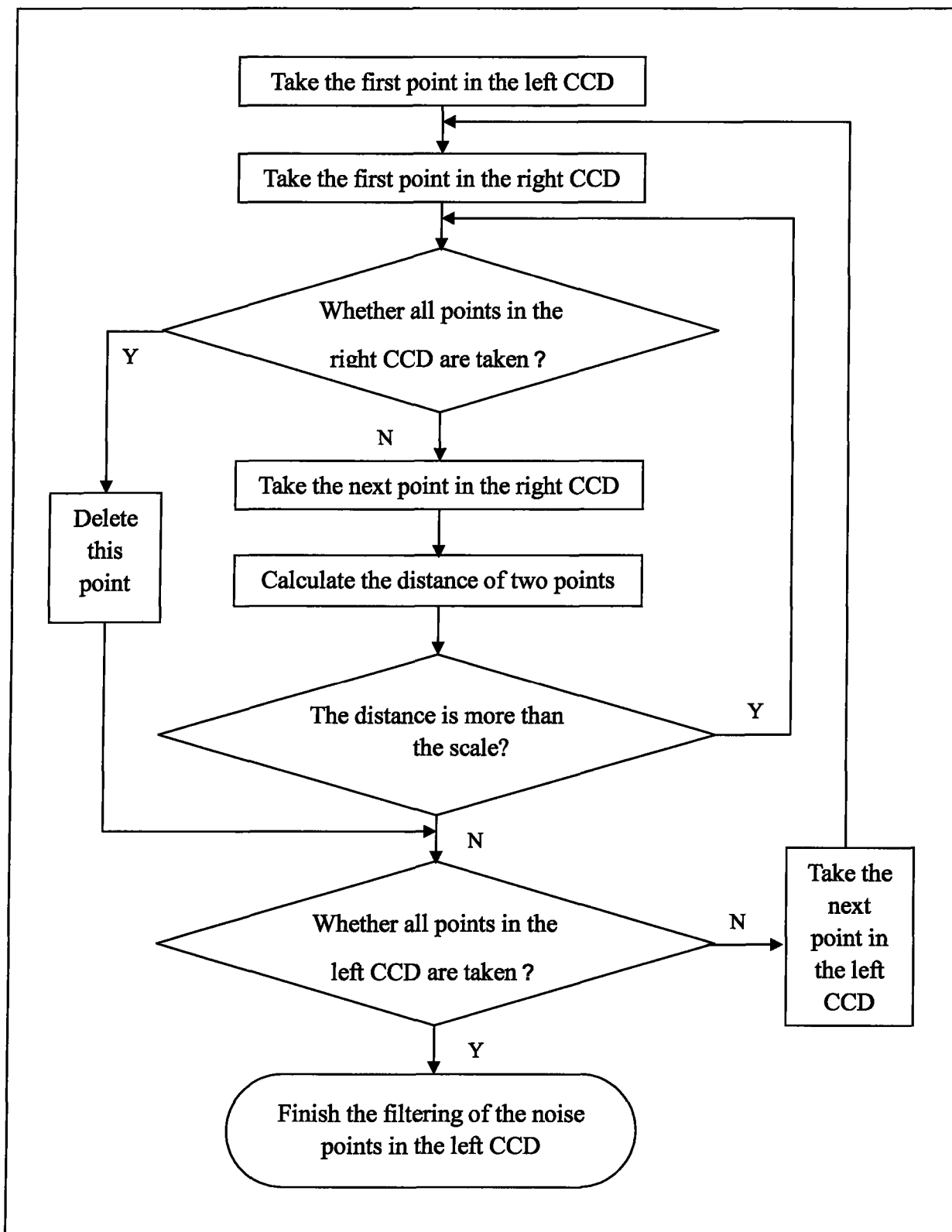


Figure 5-1 the flow chart of the filtering noise points in left CCD

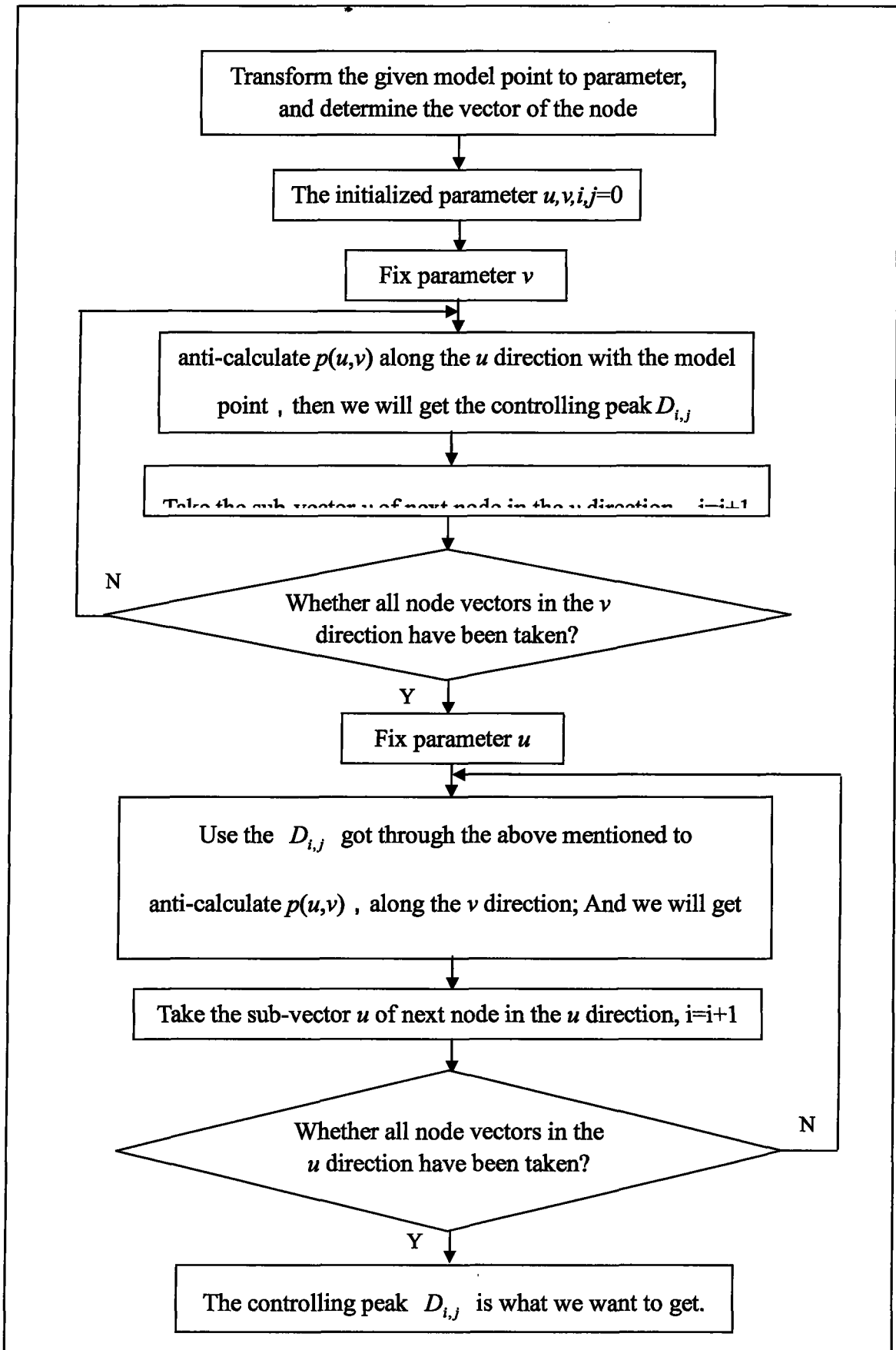


Figure 5-2 the flow chart of surface fitting using NURBS

(5) Judging whether the object is qualified

We should give an acceptable form error scale in advance. If the value of error we got through calculation is within the given scale, we regard it qualified; if it is out of the given scale, it is not qualified. This acceptable form error scale can be adjusted according to the requirement of the precision.

5.2 Analysis of the Experimental Result

In order to test the precision of the system, Tianjin Measurement Center has checked this system. We test the standard sphere with the semi-diameter of 20.007mm for ten times. The measured result is shown in the table 5-1:

Number	Form error (mm)
1	0.016
2	0.013
3	0.011
4	0.019
5	0.021
6	0.010
7	0.015
8	0.013
9	0.012
10	0.012

Table 5-1 the results of experiment for the standard sphere

According to the data offered by Tianjin Measurement Center, we can make sure the hardware's precision of the 3D laser scanner we use can fulfill the thesis's request, so we can use the points produced by the scanner to study the thesis and prove the result.

The following is the figure of the 3D laser scanner in the experiment.



Figure 5-3 the experiment of 3D laser scanner

Using the double CCD laser scanner to scan the object, we get a lot of primary points. The following figures show the position of the points produced by the scanning software designed by the two previous researchers. Figure 5-4 shows the position of the

plane points. Figure 5-6 shows the position of the standard sphere points. Figure 5-8 shows the free surface points.

The software can show the points in the form of the value of x -axis, y -axis and z -axis. We extract the 3D data of all points, and then filter the noise points by using CCD filtering algorithm, and then take off the noise points. The rest are the points we use in the program. We can use the 3D data of these points to calculate the form error.

We collect the actual value of x -axis, y -axis and z -axis to calculate form error by the program automatically, and then we can get the following results: The user interface is shown as following. In the user interface, the specific value of x -axis, y -axis and z -axis of points used in the program can be shown. In the process of the operation of the program: 2653 points used by the plane testing, 2689 points used by standard sphere testing, and 2732 points used by free surface testing. Figure 5-5 shows the result of the plane testing. Figure 5-7 shows the result of the standard sphere testing. Figure 5-9 shows the result of the free surface testing.

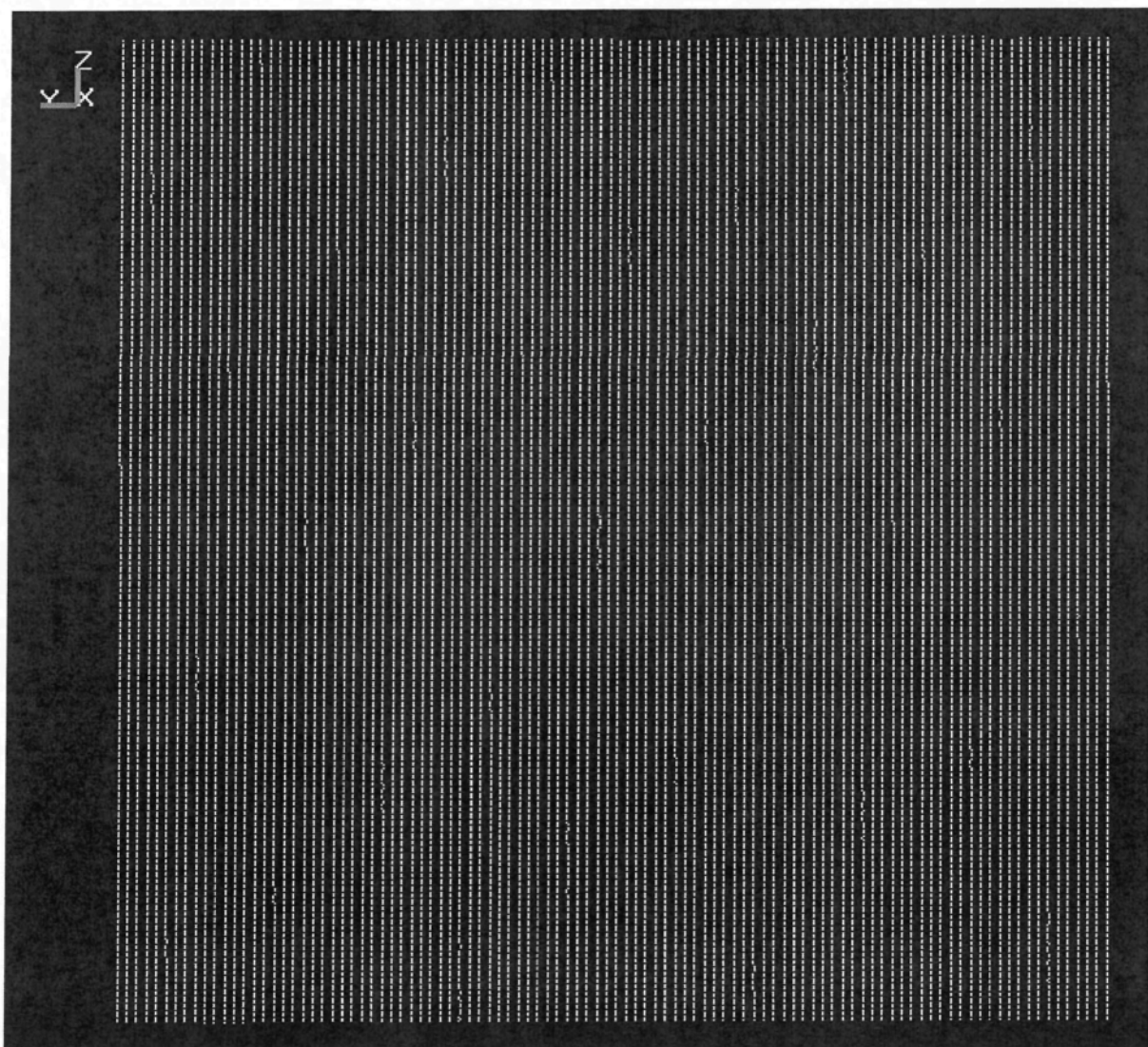


Figure 5-4 the position of the plane points

Display Form Error

Information of points

X	Y	Z
19.862	200.503	49.805
20.784	200.503	50.867
21.925	200.503	51.953
23.274	200.503	53.062
21.558	201.001	23.728
20.490	201.001	24.828
19.567	201.001	25.902

Information of standard surface

The form of surface:

Information of form error

The form error scale(mm):

Form error (mm): Eligible or not:

Figure 5-5 the result of the plane testing

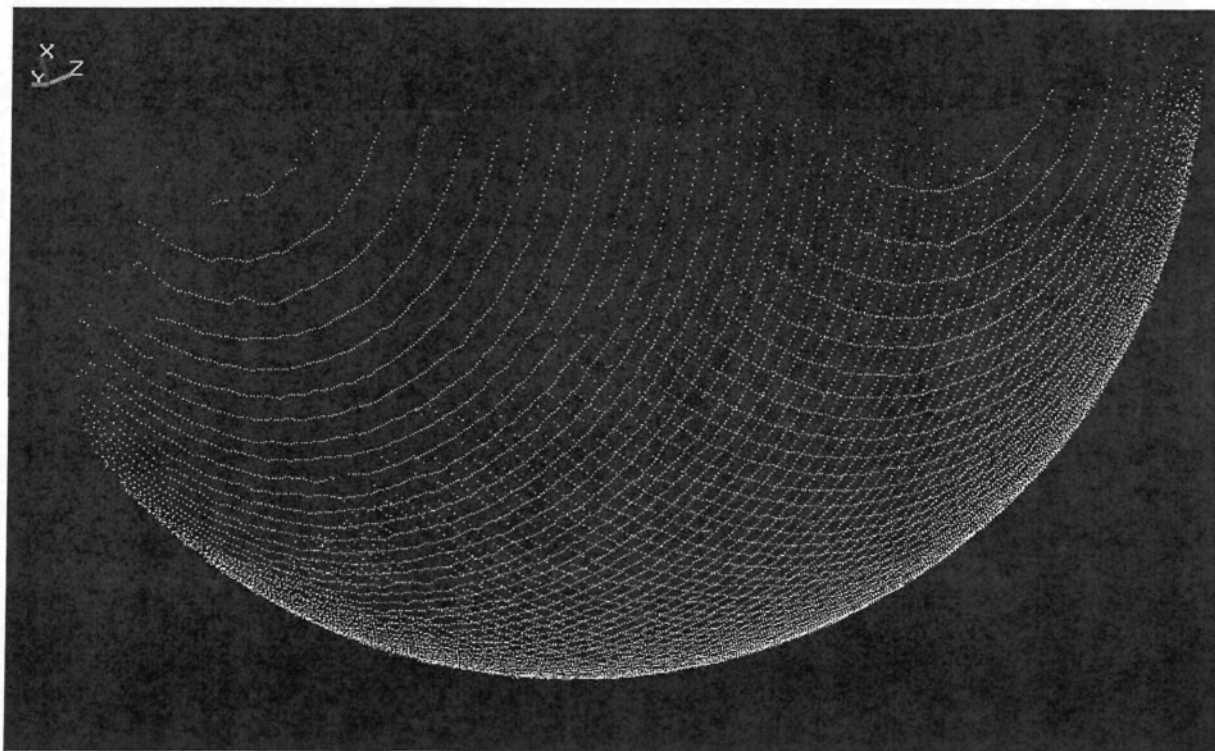


Figure 5-6 the position of the standard sphere points

Display Form Error

Information of points

X	Y	Z
48.428	210.024	51.921
47.295	210.024	52.934
48.611	209.524	23.728
49.500	209.524	24.732
50.356	209.524	25.758
51.082	209.524	26.824
51.757	209.524	27.916

Information of standard surface

The form of surface: Sphere

Information of form error

The form error scale(mm): 0.02

Form error (mm): 0.016 Eligible or not: YES

calculate cancel report

Figure 5-7 the result of the standard sphere testing

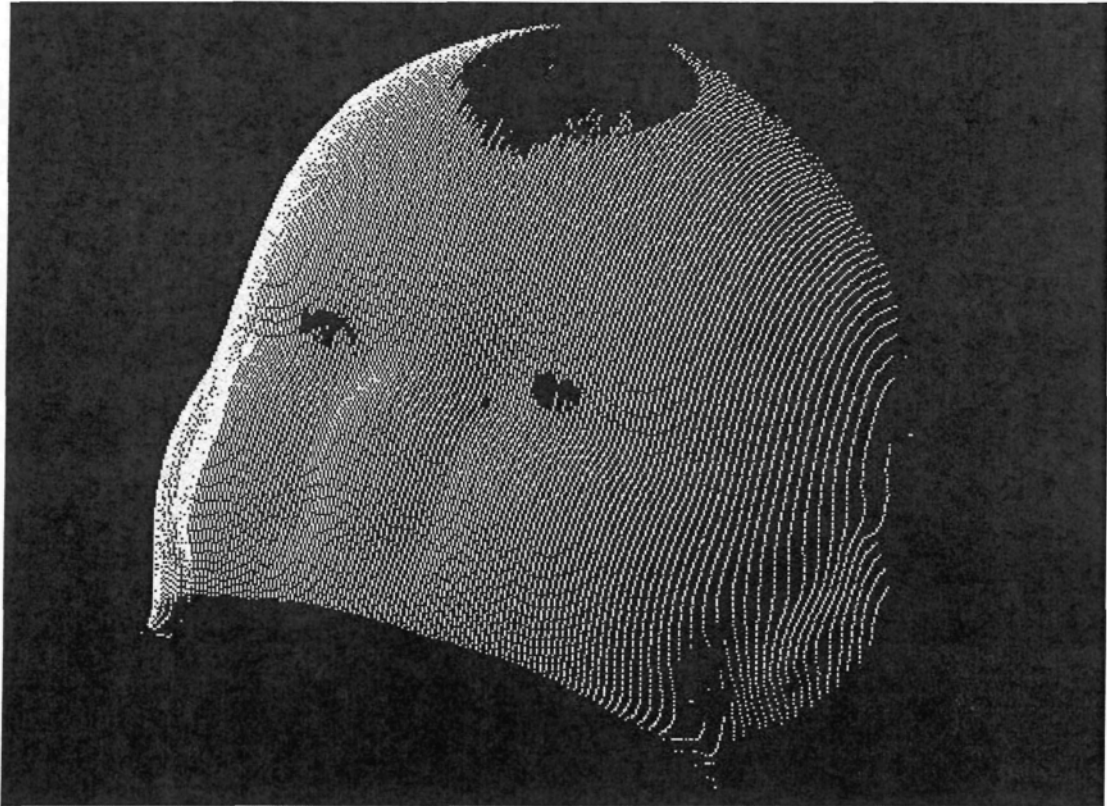


Figure 5-8 the position of the free surface points

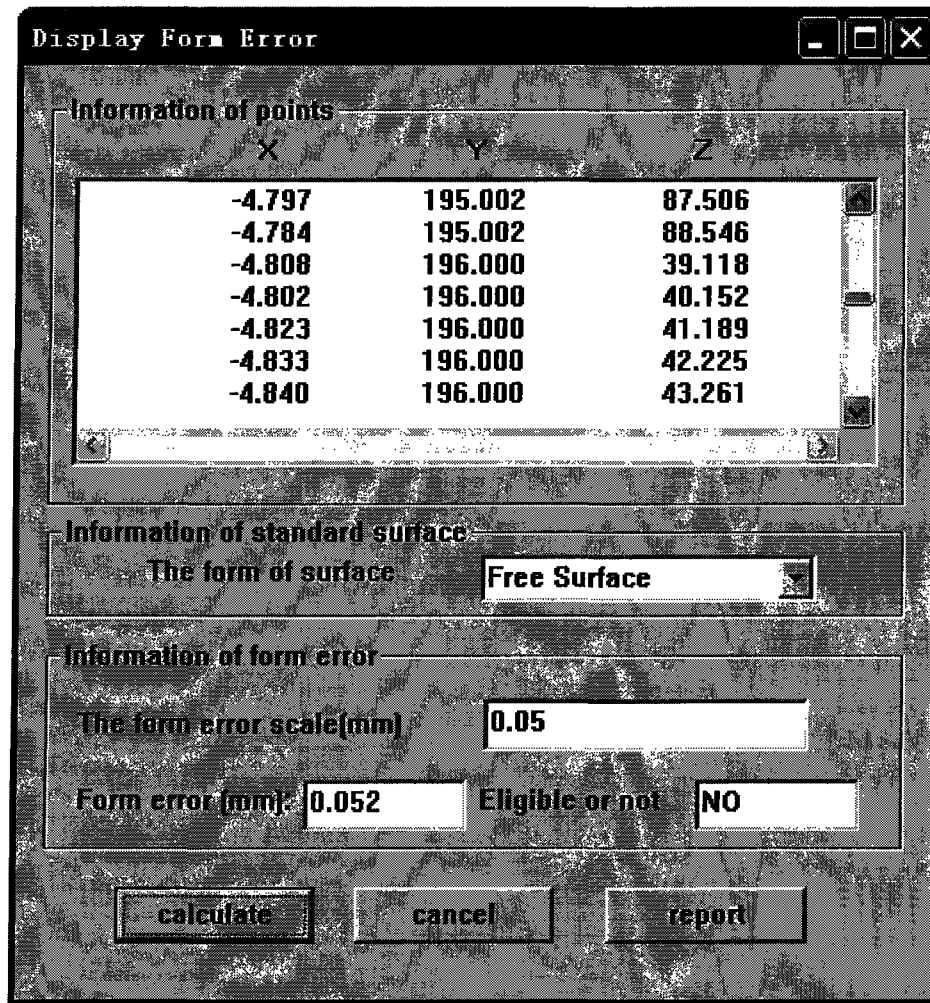


Figure 5-9 the result of the free surface testing

The experiment proves that the system can meet the requirement of the precision in the industrial production and the final aim of this project has been made true.

5.3 Summary

In this chapter, we use the computer to design software to realize the automatic

testing with the theory and algorithm introduced above. And the user interface has been given. Through the analysis the result of experiments, we can see that this system is reliable.

CHAPTER 6

THE CONCLUSION AND THE PROSPECTS

6.1 Conclusion Remarks

The reconstruction technology from the three-dimensional measured data points of an object plays an important role in the fields of industrial testing, quality control and machine vision. It is also an important method for scientific research on the aspects of science analysis, industrial control, the biological and medical fields, the material science, and so on. In recent years, with the wider application of industrial automatization and 3D laser scanning technology, product testing has become an indispensable and important link in industrial production. Many disciplines such as optics, measurement, and mathematics and computer science are involved in this thesis, from computer graphics, tolerance and technology measuring, software engineering, etc. Using the methods of NURBS surface fitting, the Least Region Principle and the Genetic Algorithm, this thesis developed a set of software tools for automatically implementing a series of process from measuring to error calculation as well as for the automatic computation of the form error of a three-dimensional object thereby solving the difficulties of computer measuring and testing.

A great number of experiments proved the reliability of the system. The research will facilitate the development of industrial automatization to a great degree, and meanwhile, it can be applied in many science research fields such as artificial intelligence.

The tasks of the research mainly includes two aspects, i.e. researching a mass of relevant theories and literatures, and according to the feature of this system and the research emphasis, selecting the most appropriate algorithms and theoretical foundation. On the basis of experiments, discussing the factors affecting the results, and then in the process of system realization, especially in the process of the realization of software, paying full attention to these affecting factors and improving on them. The main research areas covered were the following:

➤ Data collection

Use the thesis-designed measuring system to scan an object, and store the information of the object into the computer in the form of three-dimensional data points for the use in the following work.

➤ Noise point filtering

Before surface fitting, we considered that, when using one CCD to measuring the object, there are some parts that cannot be measured due to the shape of the object. In order to solve this problem, we use double CCD to measure. But when using double CCD to measure, noise point will appear. To increase the precision, these noise points must be

filtered out. This thesis puts forward a new method of filtering the noise points, i.e. comparing the point information measured by left CCD and right CCD in turn, and taking some scale as the judging condition to determine whether the point should be delete, in order to filter noise points. The research and analysis of experimental results prove that the precision is increased with noise point filtering.

➤ Surface fitting

Making use of the measured discrete data after pre-handling, i.e. noise point have been filtered, there arose the need to use a proper fitting algorithm to fit these points to a surface. There are many methods of fitting surface, for example, Cubic Spline method, Bezier method and B-Spline method and Non-uniform Rational B-Spline method (NURBS), and so on. Compared with the other fitting methods, NURBS surface fitting has excellent characteristic such as good continuity, smoothness, imitating invariability, clairvoyance invariability and part control, and so on. It is a kind of power geometric tool used to design, analyze, and handle surface. Because of its high flexibility and precision the NURBS method to describe the surface was used.

NURBS is the only method of the free curve and surface in the STEP^[60] standard. NURBS provides a uniform mathematical form for the surfaces of any shape. Through NURBS, it is possible to design the surfaces of any shape, suitable for fitting free curve and surface, especially the free curve and surface containing round and hyperbola.

In this thesis, the methods of all kinds of surface fitting are compared and finally we determined to use the NURBS method to fit the free surface. And the reconstruction of the surface can be realized.

➤ The mathematic model of form error

In order to make the standard surface and the actual measured points achieve the best matching state, the measured point must be translated and rotated. This thesis, making use of geometric invariability, deduces the coordinate relation of the measured surface, and according to the actual situation, confirms the value scope of each transformed parameter.

The Least Region Method is the best method of assessing form error of a curve or a surface. Therefore, this thesis, according to the assessing principle of the Least Region Method, established the mathematic model describing standard parameter equation surface. It is difficult to describe the surface with complex and anomalous shape using mathematic model. This thesis, on the basis of NURBS surface fitting and Least Region Method, deduces the mathematic model of the form error of the complex surface.

➤ Designing algorithm to calculate the form error

The Genetic Algorithm of unitary real number encoding, in the process of solving, makes the position of the measured surface and the standard surface achieve the best matching state, that is, the distance of the two standard surfaces that can contain the measured surface achieves the smallest distance. It satisfies the assessing standard of the

Least Region completely and the calculation precision is very high. Therefore, it is very suitable for the calculation of the form error of the standard parameter equation and the complex surface.

The Genetic Algorithm of unitary real number encoding is a new way for the standard parameter surface and the measured data handling of the complex surface, especially suitable for calculating the form error of the measured object in the three-coordinate measuring machine. It has important application value.

➤ Software design

In the thesis a complete system was designed and implemented using Visual C++ 6.0 [40][47]. Based on the theory of Software Engineering and software system structure, it combined all the theoretical components and algorithms mentioned above. In the thesis is also to be found a complete implementation that allows for an automated calculation of the form error of the measured object, which can automatically judge the quality of a product. It realizes the on-line measuring and testing in the industrial production cycle, the main objective of the thesis.

➤ The analysis of the experimental data

We do experiments repeatedly on the standard pieces like standard sphere provided by Tianjin Measurement Center. From the analysis of the experimental data it was concluded that the precision of this system achieved satisfactory results so that the aim of

the thesis was achieved.

After the gradual realization of the above steps, we can make the following

Concluding remarks:

- In the double CCD measuring system, using the method of comparing double CCD point one by one to filter the noise points can increase the system precision.
- Considering the powerful function of the NURBS surface, the thesis mainly studies the fitting algorithm of the NURBS surface. The NURBS surface fitting system provided in this thesis can flexibly design surfaces with various shapes, and it has the characteristics of stable and quick-speed calculation. It provides a practicable method for the research on the computer three-dimensional figure technology and the surface reconstruction.
- The Genetic Algorithm can find the overall optimizing solution but not get in the part optimizing solution. It is the powerful tool of parameter estimation and optimization. The thesis used an improved Genetic Algorithm, i.e. the unitary Genetic Algorithm. Its performance was deemed highly acceptable. Moreover, the Genetic Algorithm can be applied to other problems involving parameter estimation and optimization of other surface fitting. The process of biology evolution in the natural world is very one. The Genetic Algorithm is the algorithm imitating the evolution of biological organism. Therefore, improvement of the Genetic Algorithm is expected to continue. To different problems, it should explore many kinds of improved methods of the Genetic Algorithm to solve the

optimizing solution of the problems.

➤ We finally achieve the aim of this research by using the noise points filtering to increase the precision, making use of the NURBS surface fitting, combining Least Region Principle, and using the improved Genetic Algorithm. The thesis designs a reliable on-line testing system satisfying the precision of industrial production. It realizes the completely automatic process from product measuring to judging whether the product is qualified or not, and solves the difficult problem at present constraining production efficiency and the product quality in industry.

6.2 Prospects

Objects in the natural world are all three-dimensional. But general photography system can only preserve and record the three-dimensional object in the form of two-dimension, losing much three-dimensional information. With the quick development of computer technology, the memory capacity and calculating speed of computer have increased to a great extent. Technology of 3D scanning demands handling a great deal of data. So the development of computer technology provides the prerequisite for the development of the 3D scanning technology. The aim of three-dimensional visual testing is to extract the three-dimensional information of the object and digitize this information in order to make it emerge again on the computer and do some relevant handling.

The method and algorithm of this research can be used in the field of machine

vision. The machine vision means to realize the vision function of human being with computer, which is, realizing the identification to the objective world by computer^[22]. According to our present understanding, the feeling part of the human visual system is the retina. It is a system of three-dimensional sampling. The visible part of the three-dimensional object projects onto the retina. According to the two-dimensional image projected onto the retina, people can infer this object as three-dimensional. The so-called three-dimensional understanding means the understanding of the shape, size, the distance away from the observing point, character and movement feature (direction and speed) of the observed object, and so on. Machine vision means using machine to measure and judge instead of human eyes. The input device of machine vision system is usually camera and laser, taking the image of three-dimensional object as input source, that is, what is input into computer is the two-dimensional projection of the three-dimensional objective world. The machine visual system needs to reconstruct the three-dimensional objective world according to the two-dimensional information. The process is the surface fitting process.

At present, in the developed countries such as the European countries, in America and Japan, the three-dimensional scanning testing technology has been used widely in the fields of industrial manufacturing^[8], game entertainment^[32], and medicine^[59], and so on, allowing for tremendous technology advances and . Its application is in the ascendant tendency. And the manufacturers explore the products with better quality continuously. So

it can be said that the appearance of the three-dimensional scanning testing technology inaugurates a new era of the science and technology development.

Nowadays, for all kinds of products, moulds, automobile parts, handicrafts and rapid prototyping, such as precise manufacturing products, industrial sculpt design, body figure measuring like face picture, artificial shins, and teeth modules, complex carving surface measuring, solid carving, and so on, all these need to get the three-dimensional coordinates of the object. And then it is possible to finish the designing and manufacturing of the products in the shortest time. All these promote 3D scanning and testing technology making this type of research a very viable field.

The testing of the three-dimensional coordinates can be divided into contact measurement and non-contact measurement. Generally speaking, contact measurement has higher testing precision and the measurable scope is larger but the speed is slow. The data got by measurement can be right only after the semi-diameter compensation of probe. It takes a very long time to measure and the object is easy to be distorted with the pressure, which will damage the surface of the measured object.

Non-contact measurement is, according to all kinds of different visual testing technology, to obtain three-dimensional data from the measured surface or the environment. Its testing speed is much faster than that of contact measurement and it can test objects that are soft or whose shapes are easy to be destroyed. And these objects are hard to be

measured by the general contact measurement. Non-contact measurement will not damage the surface of the object.

Nowadays, with the quick development of laser technology, measuring technology and computer technology, the laser measuring technology has been more and more concerned. More and more universities and companies in the world are engaging in the measuring research. They play an important role in promoting the development of the measuring technology. The measuring technology is both advance and practical. In recent years, these technologies are applied widely in industry, especially engineering manufacturing. Laser measurement has many advantages, such as fast speed, strong anti-jamming power, no damage to the object and so on. With the development of the computer science, the level of automatization of industrial production has been increased. In industrial production, the product testing has become an important and indispensable link. The product quality is the fundament for the enterprises. Therefore, it is especially important to discover the unqualified products in time. But both precision and speed of the traditional artificial testing method cannot keep up with the development of the industrial automatization. The many advantages of synchronous measurement provide precondition for the automatic measuring of the products, which enables to realize the on-line dynamic measuring and testing. This is the aim of this research. It will speed the development of the modern measuring technology. We can realize the automatic measuring and testing with

the help of measuring technology, mathematic and computer technology.

In the following, I will enumerate some typical application of this research:

➤ In the large production of modernization, visual testing is usually an indispensable link. For example, the appearance of the automobile parts, the right and wrong of the medicine package, the quality of the IC printing, etc., all these need many testing workers who observe and testing them with eyes or with the help of the microscope. Artificial testing not only affects the efficiency, but also brings the trustless factors, which will directly affect the product quality and cost. Besides, many testing procedure not only demands the testing of the appearance, but also needs to get the testing data correctly, such as the width of the parts, the diameter of the hole and the coordinates of the datum mark, and so on. It is different to finish this work quickly by human eyes. The laser scanning technology developing fast in recent years solves this problem. Compared with artificial vision, the best advantage of laser scanner is precise, fast, reliability and digitize.

The manufacturers always wish to increase the efficiency of the products and manufacture various products to meet the demands of different customers in order to enhance competitiveness; therefore, this helps the quick development of laser scanning measuring testing technology and quick shaping technology. Laser scanning measuring technology can get the information points of the measured objects through measuring machines, and then reconstruct the CAD model. In this way, it is possible to design this

model with the computer, and transfer to CAM software quickly, and put it into production. It has many advantages using laser scanning measurement system to measure the three-dimensional object, such as easy automatization, high measuring efficiency, quickness, non-contact, strong anti-jamming power, and so on. Due to these advantages, it has been widely applied in many fields like mechanical manufacturing. Besides, to save human cost and to test and classify the products on the product line, it is often needed to use laser-scanning system to get the information of the three-dimensional object. Therefore, this research will be engaging in increase the precision of laser scanning measuring and apply it into the on-line dynamic measuring and testing. It will make full use of the advantages of laser scanning measurement and increase the quality of products, find the waste, reduce the production cost, shorten greatly the time of putting the products into the market.

- In the actual application, especially the reverse engineering^[50], we get a series of discrete data after digitize this work-piece measuring. In order to realize the reprocessing of the work-piece or the error assessing, it is needed to reconstruct curve and surface precisely with these discrete data. In the modeling domain, B-Spline, especially NURBS has become one of the basic modeling theories for curve and surface with its excellent characteristic. It has great importance to use NURBS to model curve and surface.
- In the model-manufacturing field, this research has wide application foreground.

One of the main reasons for the invalidation of the model is the serious abrasion on the surface of the model antrum^[55]. The reparation of surfaces of all kinds of antrum has become a problem that must be solved. The NURBS surface fitting has excellent characteristic with good continuity, smoothness and clairvoyance invariability, and so on. Therefore, it is very suitable for analyzing the shaping rule of model antrum. Thus, we use NURBS surface fitting to construct model antrum. Its point data can be measured from the existent model antrum. Then analyze the shaping rule of the model antrum, and then the abrasion on the surface of the model antrum can be amended precisely.

➤ This research can be also applied in many aspects of the science research. In scientific research, the on-line measuring and testing can be used, such as the field of the artificial intelligence. In recent years, the research of the artificial intelligence has developed quickly, because the robot can not only finish the dangerous task, but also can help and serve human being. In the scientific research and daily life and work, the robot can do the following work specifically: working at height, heavy manual work, the investigation and search for all kinds of disaster scene, toxic operation, space research and industrial production and housework, etc. Nowadays, the robot has become the partner and assistant of human being. As is known to all, the robot can handle data only with the help of computer. Therefore, the observed object is stored in the computer in the form of point data through the laser scanning. But it cannot simply reflect the characteristic of the object

according to these measured discrete points. Of course, it cannot understand the object. Thus, it needs to handle these discrete points in order to reconstruct the shape of the observed object^[52].

- In the field of medicine, the organ, and blood vessel, etc. can be reconstructed with three-dimension measuring and fitting in order to help the doctors to analyze illness more precisely.
- In the field of traffic surveillance, it is usually used in the investigation of traffic accidents, car surveillance, vehicle identification, car number identification and detecting and tracking the “suspected” target.
- In the field of security identification, according to the image characteristic of face, eye-ground and fingerprint, and so on, it can identify the special person.
- In the field of car navigation, it can be applied in identifying targets, roads, and judging barriers, and so on. This technology has been applied in vehicle with no person, aircraft with no person, and chariot with no person, and so on.
- The above only introduces the typical application of this research. In a word, this research can benefit many fields, including the following aspects: automobile manufacturing, communications industry, home appliances, toys, aerospace industry, the hardware industry, optical industry, sport equipment industry, and so on. It can also be applied in the many scientific fields such as artificial intelligence, meteorology, geological

exploration and mining, medicine, graphics and national defense, and so on. Especially in the industrial production, the research has very wide developing foreground.

6.3 Future Work

From the concluding the whole developing process, we discovered that the following areas could be improved so has to increase the speed and precision:

- What this research realizes is the scanning of some part of the object. There is no research on the large work-piece scanning. If we want to scan the large work-piece, it is needed superposition handle for the scanned data.
- To scan an object completely, it is needed to realize the 360° scanning of the object. How to realize it and guarantee the scanning precision is needed to be researched in the further.
- In the following research, if we want to enlarge the scope of the scanning and increase the precision of the scanning, it can use CCD with better resolving power, the lens with higher precision and thinner line laser.
- In the aspect of the algorithm, it can seek controlling parameters such as better population size, cross-probability, variability probability, the greatest evolutionary generations, and so on, in order to make the system with higher precision.
- In the aspect of software design, it can strengthen the maneuverability and make

software to be used easier and more convenient.

At present, although the laser scanning technology is not so perfect, and the application of the three-dimensional measurement is limited, I believe that with the further improvement of visual theory and computer technology, the three-dimensional laser scanning measuring and testing technology will have greatly wide application foreground.

BIBLIOGRAPHY

- [1] Be Boor C. On Calculation with B-Spline. *Approx Theory*, 50-62, 1992.
- [2] Berzins V , Accuracy of Laplacian Edge Detections[J] , *CVGIP* , 195-210,1984.
- [3] Be Boor C. B-Spline Interpolation. *Math and Phy*, 211-281, 1962.
- [4] Be Boor C, Lynch R E. On spline and their Minimum Properties. *Math Mech*, 953-969, 1966.
- [5] Cai-Yiheng. Approaching Linear Programming Method, A New Method to Evaluate Form Errors. *Journal of Beijing Polytechnic University*, Vol.25, No.3, Sep, 1999.
- [6] Canny J F , A Computational Approach to Edge Detection[J] , *IEEE Trans on PAMI* , Vol.8, No.6, 679-698, 1985.
- [7] Cao-Lixin, Yong-Hong. Smooth Fitting Based on the B-Spline. *Mechanism*, Vol.41, No.467, China, Jul.2003.
- [8] Chen-Lihong. The Research and Development of the Machine Vision. *Zhejiang University, China*, Mar.2003.
- [9] Cheng-Liangqing, Wang-Longsan, Wang-Qiaoguan. The Precision Analysis of the Free Surface of NURBS. *Agriculture Machine*, Vol.37, No.3, China, Mar.2006.
- [10] Daugman J G. High Confidence Visual Recognition of Persons by a Test of Statistical Independence . *IEEE Tran . Pattern Machine Intel*, Vol.15, No.2, 1148-1161, 1993.
- [11] DaVies E R . A Modified Hough Scheme for General Circle Location ,*Pattern Recognition Letters* , 37-43, Jul,1987.
- [12] Ding-Ru. Algorithm of NURBS Surface Fitting and its Application. *Journal of Tianjin University of Technolohg and Education*, Vol.14, No.4, China, Dec, 2004.
- [13] Donald Hearn, M.Pauline Basker. *Computer Graphics*. Publishing House of Electronics Industry. May.2002.
- [14] Etter D M, Hicks M J, Cho K H. Recursive Adaptive Filter Design using an Adaptive Genetic Algorithm. *Proc IEEE Inf Conf ASSP*, 635-638, 1982.
- [15] Etter D M, Masukaw M. A Comparison of Algorithms for Adaptive Estimation of the Time Delay between Sampled Signals. *Proc IEEE Int Conf ASSP*. 1253-1256,1981.
- [16] Feng-Guoxin. The Measurement and Modeling of the Free Curve and Surface in the Field of Reverse Engineering. *Tianjin University Press*. Tianjin, China, 1998.
- [17] Feng-Guoxin, Zhang-Guowei, Xie-Xiao. Model Buliding of Free Curve with the

- Least Approximate Error Based on B-Spline. *Journal of the Tianjin University*, Vol.34, No.3, China, May.2001.
- [18] Goldberg D E. *Genetic Algorithms: in Search Optimization and Machine Learning*. Addison-Wesley Press, 70-84, 1989.
- [19] Han-Zuxing. *The Optimization Algorithm of From Error*. *Measurement Technology*. Vol.13, No.4, 245-249, China, 1992.
- [20] Holland. *Adaptation in Nature and Artificial System*. Cambridge, MA: MIT Press, 1992.
- [21] Hou-Yu. *The Theory of Assessing of Form Error*. *Measurement Technology*. Vol.17, No.1, 70-73.China, 1996.
- [22] Hui-Zenghong. *The Techonology of the Measurement and Reconstruction of the 3D Object using the Laser Scanner*. Northwest Industry University. China, May.2005.
- [23] Jiang-Dawei, Wang-Ziran. *The Method of Complex Surface Fitting*. *The Technology of Avigation Calculation*, Vol. 29, No. 2. China, Jun. 1996.
- [24] Jin-Lizuo. *The Method of Image Dividing of Self-adaptation Scale[j]*. *Journal of Graphics and Image*, Vol.5, No.5, 390-395, 2000.
- [25] Lai-Xinmin, Huang-Tian, Zeng-Ziping. *Based on the Discrete Point Data to Reconstruction Surface using NURBS*. *Computer Design and Graphics*, Vol.11, No.5, 433-436, China, 1999.
- [26] Lin-Yibin. *A Study of 3D Profile Measuring Based on Laser Detecting*. Tianjin China, 2005.
- [27] Liu-Dingyuan, Zhao-Yuqi, Zhan-Tingxiong. *Fitting Method of Bezier and B-spine*. *Calculation Mathematics*, Vol.6, No.4, 360-365, China, 1984.
- [28] Liu-Guixiong. *Dividing of Image based the Hough Transformation*. *Optics Engineering*. Vol.6, No.3, 257-260, China, 2006.
- [29] Liu-Jian, An-Libang. *The Theory and Appliance for the Form Error Contain*. *Measurement Technology*, Vol.13, No.1, 24-32, 1992
- [30] Liu-Wenhai, Wang-Renhong. *A Method of Modification of NURBS Surface*. *Application Mathematics*, Vol.16, No.2, 107-111, China, 2003.
- [31] Microsoft Corporation. *Design Program Using Microsoft Visual C++ 6.0 MFC (translation edition)*. Tsinghua University Press , China, 2002.
- [32] Milan Sonka. Vaclav Hlavac, Roger Boyle. *Image Processing, Analysis, and Machine Vision*. Publishing House of the Post. Beijing, China, 2003.
- [33] PETAL S. *Threshold Selection using Reny's Entropy*, *Pattern Recognition*, Vol. 30, No.1, 71-84,1997.
- [34] Ran-Guanzhi, Chen-Xunchun, Lian-Kai, Dong-Yunhan, *The Applied Technique and Familiar Programs of Visual C++ 6.0*, China Machine Press, 264-283, Beijing, China,

2003.4.

- [35] Shi-Fazhong. CAD and NURBS. Beijing Savigation Press, China, 1994.
- [36] Smith S M , Edge Thinning used in the SUSAN Edge Detector[R] , International Technical Reports TR95SMS5 , Defense Research Agency , Farnborough , Hampshire , GV146TD , UK , 1995.
- [37] Special Report , Digitize and the Reverse Engineering, CAD/CAM and Manufacturing, 83-85, Jul.2003.
- [38] Tang-Zesheng. Vision of 3D Space. Tsinghua University Press, Beijing, China, 1999.
- [39] Wang-Ning, Guo-Li, Jin-Dasheng. The Using of Genetic Algorithm in the Field of Static Data Relevancy of Multi-sensor and Multi-target. Data Collection and Solving. Vol. 14, No.1, 18-21.1994.
- [40] Wang-Guan. The Instance of Visual C++ 6.0. China Machine Press. China, Feb.2002.
- [41] Wang-Shengfu, Jiang-Dawei. Spline Function and Appliance. Northwest Industrial University Press, China, 1989
- [42] Wang-Shu.The Reconstruction of Laser-based Real-time Machine Vision Measuring Data. Tianjin, China, 2005.
- [43] Woodward C D. Cross-sectional Design of B-Spline Surface. Computers and Graphics, Vol.11, No.2, 193-201, 1987.
- [44] Woodward C D. Skinning Techniques for Interactive B-Spline Surface Interpolation. CAD, Vol.20, No.8, 441-451, 1988.
- [45] Wu-Jiankang. The Analysis of Digital Image [M], Publishing House of the Post, Beijing, China, 1989.
- [46] Wu-Wei, Luo-Liangling, Tian-Hua, The Research for the Space Curve's Direct Interpolation Arithmetic. Journal of Nanchang University, Vol, 26, No.3, China, Sep, 2004.
- [47] Xi-qing, Zhang-Chunlin. The Programming Technology of Visual C++ 6.0. China Water Technology Press. China, 1999.
- [48] Xiong-Youlun. The Mathematic Method of the Measurement Precise. China Measurement Press, China, 1989.
- [49] Xiong-Zhenxiang. Smooth Fitting of the Surface. National Defence Press, Beijing, China, 1979.
- [50] Xu-Zhiqin, Sun Chang-ku. The 3D Reserve Engineering. China Measurement Press. Beijing, China, Apr.2002.
- [51] Yao Leehter, Sethares W A. Non-linear Parameter Estimation via the Genetic

- Algorithm. IEEE Tran on Signal Processing, Vol.42, No.4, 927-935, 1994.
- [52] Yu-Yang, Huang-Weiyi. Based the Marr Theory, the Research of Robot that can identify the Face of People. 108-111,2003.
 - [53] Yuan-Jie. Using the Hough Transformation to Distill the Inflexion of Image. Wuhan University, Vol.1, 85-88, China, 1998.
 - [54] Yuan-Qisun. Calculation of Shaping Geometry. Savigation Industry Press. Beijing, China, 1987.
 - [55] Zeng-Shanqi, Zheng-Mei. Die Cavity On-line Fit with Cubic Spine Function. Machinery Design and Manufacuture, May.2006.F
 - [56] Zhang-Huijuan, Zhou-Hongyu, the Application of Scanning Technique.Technique Industry, Dec. 1995.
 - [57] Zhou-Xiaoping, Xu-Shejiao. Graphics of Computer. Xian Electronics technology Industry Press. Xian China, 2005.
 - [58] Zhou-Qinfang. Technology of Measurement. Shanghai Traffic University, Shanghai, China, 2001.
 - [59] Zhou-Xinlun, Liu-Jian, Liu-Huazhi, the Management of the Digital Image [M]. National Defence Industry Press, Beijing, China, 1984.
 - [60] Zhu-Yongqiang, Lu Cong-da. The Introduction of Technology of Free Curve and Sruface. Manufacturing of China, Vol.35, No.5, 110-113, 2003.